Article

In vivo CRISPR base editing of *PCSK9* durably lowers cholesterol in primates

https://doi.org/10.1038/s41586-021-03534-y

Received: 6 December 2020

Accepted: 11 April 2021

Published online: 19 May 2021

Check for updates

Kiran Musunuru[1,2,3], Alexandra C. Chadwick[4], Taiji Mizoguchi[4], Sara P. Garcia[4], Jamie E. DeNizio[4], Caroline W. Reiss[4], Kui Wang[4], Sowmya Iyer[4], Chaitali Dutta[4], Victoria Clendaniel[4], Michael Amaonye[4], Aaron Beach[4], Kathleen Berth[4], Souvik Biswas[4], Maurine C. Braun[4], Huei-Mei Chen[4], Thomas V. Colace[4], John D. Ganey[4], Soumyashree A. Gangopadhyay[4], Ryan Garrity[4], Lisa N. Kasiewicz[4], Jennifer Lavoie[4], James A. Madsen[4], Yuri Matsumoto[4], Anne Marie Mazzola[4], Yusuf S. Nasrullah[4], Joseph Nneji[4], Huilan Ren[4], Athul Sanjeev[4], Madeleine Shay[4], Mary R. Stahley[4], Steven H. Y. Fan[5], Ying K. Tam[5], Nicole M. Gaudelli[6], Giuseppe Ciaramella[6], Leslie E. Stolz[4], Padma Malyala[4], Christopher J. Cheng[4], Kallanthottathil G. Rajeev[4], Ellen Rohde[4], Andrew M. Bellinger[4] & Sekar Kathiresan[4]✉

Gene-editing technologies, which include the CRISPR–Cas nucleases[1–3] and CRISPR base editors[4,5], have the potential to permanently modify disease-causing genes in patients[6]. The demonstration of durable editing in target organs of nonhuman primates is a key step before in vivo administration of gene editors to patients in clinical trials. Here we demonstrate that CRISPR base editors that are delivered in vivo using lipid nanoparticles can efficiently and precisely modify disease-related genes in living cynomolgus monkeys (*Macaca fascicularis*). We observed a near-complete knockdown of *PCSK9* in the liver after a single infusion of lipid nanoparticles, with concomitant reductions in blood levels of PCSK9 and low-density lipoprotein cholesterol of approximately 90% and about 60%, respectively; all of these changes remained stable for at least 8 months after a single-dose treatment. In addition to supporting a 'once-and-done' approach to the reduction of low-density lipoprotein cholesterol and the treatment of atherosclerotic cardiovascular disease (the leading cause of death worldwide[7]), our results provide a proof-of-concept for how CRISPR base editors can be productively applied to make precise single-nucleotide changes in therapeutic target genes in the liver, and potentially in other organs.

In vivo gene editing is an emerging therapeutic approach to making DNA modifications in the body of a patient (such as in the liver). Gene-editing methods include CRISPR–Cas9 and –Cas12 nucleases[1–3], CRISPR cytosine base editors[4], CRISPR adenine base editors[5], and CRISPR prime editors[8]. CRISPR base editors are an attractive gene-editing modality because they function efficiently for introducing precise targeted alterations without the need for double-strand breaks, in contrast to CRISPR–Cas9 and other gene-editing nucleases. Although there are numerous examples of in vivo editing of target genes with CRISPR–Cas9 nucleases[9–12] and CRISPR base editors[13–15] in rodent models, and clinical trials with CRISPR–Cas9 nuclease therapies are underway, to our knowledge no demonstration of the efficient delivery of a CRISPR base editor in primates has previously been described.

The *PCSK9* gene is a candidate target for in vivo gene editing. Whereas rare gain-of-function mutations in human *PCSK9* cause familial hypercholesterolaemia[16], naturally occurring loss-of-function *PCSK9* variants occur in 2–3% of individuals in some populations. These variants result in lower levels of low-density lipoprotein (LDL) cholesterol in the blood and a reduced risk of atherosclerotic cardiovascular disease, without serious adverse health consequences[17,18]. A few individuals have previously been reported to have a complete knockout of PCSK9[19,20]. *PCSK9* is preferentially expressed in the liver, and liver-specific knockdown of this gene using the small interfering RNA (siRNA) inclisiran has therapeutic effects on lipid levels that last several months in patients[21]. In principle, the one-time editing of *PCSK9* could produce an even more durable—and perhaps permanent—reduction in the levels of LDL cholesterol in the blood, and thereby markedly lower cumulative exposure to LDL cholesterol[22]; this stands in contrast to existing approved therapies (for example, statins and PCSK9 antibodies) that must be chronically taken daily or every few weeks and suffer from a lack of patient adherence[23–26].

Here we report the efficient in vivo delivery of a CRISPR adenine base editor using lipid nanoparticles (LNPs) in cynomolgus monkeys to introduce a precise single-nucleotide *PCSK9* loss-of-function mutation, which results in reductions of PCSK9 and LDL cholesterol (which remain lowered for at least eight months). These results provide a

[1]Cardiovascular Institute, Perelman School of Medicine at the University of Pennsylvania, Philadelphia, PA, USA. [2]Division of Cardiovascular Medicine, Department of Medicine, Perelman School of Medicine at the University of Pennsylvania, Philadelphia, PA, USA. [3]Department of Genetics, Perelman School of Medicine at the University of Pennsylvania, Philadelphia, PA, USA. [4]Verve Therapeutics, Cambridge, MA, USA. [5]Acuitas Therapeutics, Vancouver, British Columbia, Canada. [6]Beam Therapeutics, Cambridge, MA, USA. ✉e-mail: skathiresan@vervetx.com

proof-of-concept for the efficient in vivo delivery of base editors to the primate liver, which is a critical requirement for the development of these classes of editor for the treatment of human diseases.

Base editing in hepatocytes in vitro

CRISPR adenine base editors can induce targeted A→G edits in DNA (T→C on the opposing strand) and can inactivate genes by disrupting splice donors (a canonical GT sequence on the sense strand) or splice acceptors (a canonical AG sequence on the sense strand) at exon–intron boundaries[27] (Extended Data Fig. 1). The adenine base editor 8.8-m (hereafter, ABE8.8)[27] uses its core *Streptococcus pyogenes* nickase Cas9 protein with a guide RNA (gRNA) to engage a 20-bp double-strand protospacer DNA sequence, flanked by an NGG protospacer-adjacent motif (PAM) sequence on its 3′ end. Unlike Cas9 and Cas12, ABE8.8 does not make double-strand breaks; instead, it uses an evolved deoxyadenosine deaminase domain—fused to the *Streptococcus pyogenes* nickase Cas9—to chemically modify an adenosine nucleoside on one DNA strand, which (in combination with nicking of the other strand) enables highly efficient A•T to G•C transition mutations at the targeted site. The activity window of ABE8.8 typically ranges from positions 3 to 9 in the protospacer DNA sequence, and peak editing is observed at position 6 of the protospacer[27].

We identified 20 gRNAs that target protospacer DNA sequences with NGG PAMs that were positioned such that a *PCSK9* splice-donor or -acceptor adenine lay within the activity window of ABE8.8. For each candidate target site, we co-transfected in vitro-transcribed ABE8.8 messenger RNA (mRNA) along with a chemically synthesized gRNA[28] into primary human hepatocytes. Three of the gRNAs demonstrated a relatively high level of editing activity at the target splice site; one of these gRNAs (hereafter, *PCSK9-1*) also showed the greatest degree of orthogonality to the reference genome (that is, a lack of protospacer similarity to other genomic sequences with the potential for off-target mutagenesis) (Fig. 1a, Extended Data Figs. 2, 3, Supplementary Table 1). The *PCSK9-1* gRNA targets the splice donor at the boundary of *PCSK9* exon 1 and intron 1 (with a target adenine in position 6 of the protospacer), the disruption of which is predicted to result in retention and read-through of at least part of intron 1, adding amino acids to the portion of PCSK9 that is encoded by exon 1. However, owing to the presence of an in-frame TAG stop codon near the beginning of intron 1, the protein would terminate after the addition of only three amino acids (Extended Data Fig. 1c).

For delivery to human hepatocytes, we used previously described methods[29,30] to formulate LNPs that contained ABE8.8 mRNA and *PCSK9-1* gRNA at a 1:1 ratio by weight. We treated primary human hepatocytes with LNPs, which resulted in over 60% base editing of the splice site at a range of doses (Fig. 1b, Extended Data Fig. 1c). The *PCSK9-1* gRNA has a perfectly matched protospacer DNA sequence in the cynomolgus monkey orthologue of *PCSK9*, and the same LNPs produced a high level of splice-site editing in primary cynomolgus monkey hepatocytes (Fig. 1c). Reverse transcription–PCR of mRNA from treated primary human hepatocytes (using primers in exon 1 and exon 2) confirmed that splice-site disruption resulted in the use of alternative splice-donor sites within intron 1, well downstream of the in-frame TAG stop codon (Fig. 1d, Supplementary Table 2). *PCSK9* expression in treated primary human hepatocytes was reduced by 55%, consistent with nonsense-mediated decay.

Base editing in mice

At the junction of exon 1 and intron 1 of *Pcsk9* (the mouse orthologue of *PCSK9*), there is a protospacer and PAM sequence that is compatible with the use of ABE8.8 to disrupt the splice site (being homologous to the human and cynomolgus monkey sequence, but with four mismatches): we therefore tested the corresponding gRNA (designated

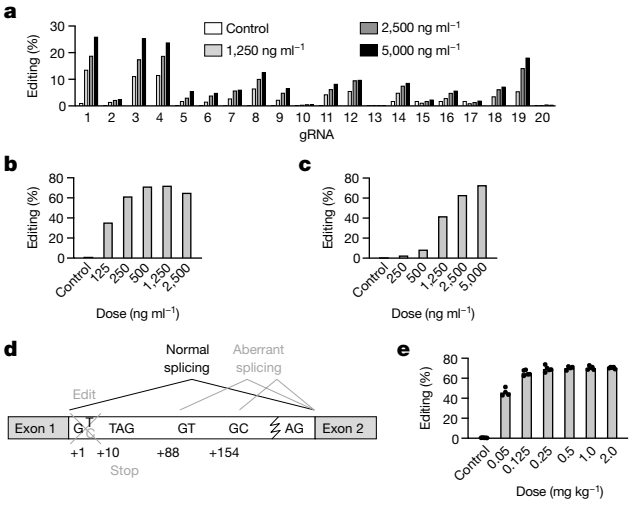

Fig. 1 | Adenine base editing of *PCSK9* in primary human hepatocytes, primary cynomolgus monkey hepatocytes and mice. a, Editing of splice-site adenine bases throughout the human *PCSK9* gene with 20 candidate gRNAs (labelled 1 to 20) in primary human hepatocytes transfected with ABE8.8 mRNA and gRNA at three different doses ($n = 1$ sample per dose). **b**, **c**, Editing of the *PCSK9* exon 1 splice-donor adenine base in primary human hepatocytes (**b**) or primary cynomolgus monkey hepatocytes (**c**), treated with different doses (ng RNA per ml) of an LNP formulation with ABE8.8 mRNA and *PCSK9-1* gRNA ($n = 1$ sample per dose). These results are replicated in Fig. 4b, c. **d**, Schematic showing alternative splice-donor sites that result from editing of the *PCSK9* exon 1 splice-donor adenine base (altering the GT splice donor to GC via editing of A on the antisense strand) in primary human hepatocytes, determined through reverse transcription of isolated RNA and PCR amplification with flanking primers in *PCSK9* exons 1 and 2. **e**, Editing of the *Pcsk9* exon 1 splice-donor adenine base in wild-type mouse liver, assessed one week after treatment with different doses (mg RNA per kg body weight) of an LNP formulation with ABE8.8 mRNA and *Pcsk9-1m* gRNA. $n = 5$ mice for control, 0.125 mg kg^{-1}, 0.25 mg kg^{-1}, 1.0 mg kg^{-1} and 2.0 mg kg^{-1} dosing groups; $n = 4$ mice for 0.05 mg kg^{-1} and 0.5 mg kg^{-1} dosing groups; bar indicates mean editing in group.

PCSK9-1m). Using previously described methods[12], we formulated LNPs that contained ABE8.8 mRNA and *PCSK9-1m* gRNA at a 1:1 ratio by weight and administered the LNPs to wild-type C57BL/6J mice via intravenous infusion at a range of doses. Upon necropsy 1 week after LNP infusion, we observed approximately 70% liver base editing of the splice site at various doses down to 0.25 mg per kg body weight (mg kg^{-1}) (Fig. 1e, Extended Data Fig. 4a–f), consistent with saturation editing of the hepatocytes in the liver (as hepatocytes comprise around 70% of liver cells).

Base editing in cynomolgus monkeys

We next assessed whether ABE8.8 could edit *PCSK9* in the livers of cynomolgus monkeys. For all cynomolgus monkey studies, we formulated LNPs that contained ABE8.8 mRNA and *PCSK9-1* gRNA at a 1:1 ratio by weight[29,30]. In a pilot short-term study, we administered LNPs to monkeys via intravenous infusion at a dose of 1.0 mg kg^{-1}, which was chosen in light of the results of the mouse study. For three monkeys that underwent necropsy at 2 weeks after LNP infusion, there was a mean 63% base editing frequency of the *PCSK9* splice-site adenine in the liver, and no bystander base edits were observed elsewhere in the protospacer; there was a mean insertion and/or deletion (indel) frequency of 0.5% (Fig. 2a, Extended Data Fig. 4g–i). The editing was accompanied by a mean 81% reduction in the level of PCSK9 in the blood, and a mean 65% reduction in levels of LDL cholesterol in the blood (Fig. 2b, c). For two monkeys that underwent necropsy at 24 h after LNP infusion, there was a mean 48% editing frequency. In assaying base editing in a wide variety

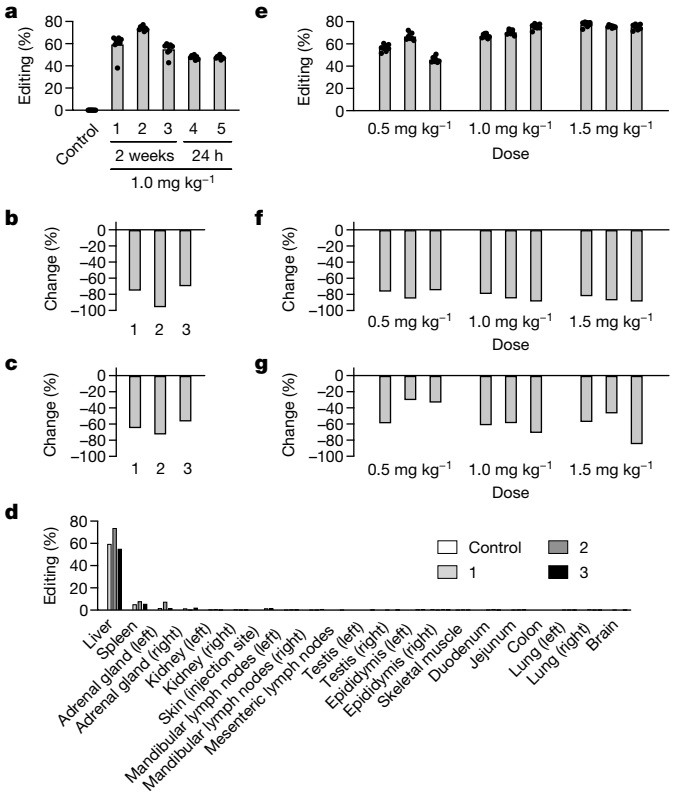

Fig. 2 | Short-term effects of adenine base editing of *PCSK9* in cynomolgus monkeys. a, Editing of the *PCSK9* exon 1 splice-donor adenine base in the livers of cynomolgus monkeys (labelled 1–5) that received an intravenous infusion of a dose of 1.0 mg kg^{-1} LNP formulation with ABE8.8 mRNA and *PCSK9-1* gRNA, with necropsy at 2 weeks (3 monkeys) or 24 h (2 monkeys) after treatment. Control, monkey that received phosphate-buffered saline (PBS) and was necropsied at two weeks. For each monkey, editing was assessed in samples collected from sites distributed throughout the liver. $n = 8$ samples; bar indicates the mean editing in the monkey. **b**, **c**, Per cent change in the levels of PCSK9 (**b**) or LDL cholesterol (**c**) in blood in the three monkeys from **a** that underwent necropsy at two weeks after treatment, comparing the level at two weeks with the baseline level before treatment. $n = 1$ blood sample per monkey. **d**, Tissue distribution of editing of the *PCSK9* exon 1 splice-donor adenine base in the three monkeys from **a** that underwent necropsy at two weeks after LNP treatment, and in the control monkey. $n = 1$ sample per monkey for each indicated organ, except for the liver; the liver data represent the mean shown in **a** calculated from eight liver samples each. **e**–**g**, Dose–response study, with liver *PCSK9* editing (**e**) and reduction of the levels of PCSK9 (**f**) or LDL cholesterol (**g**) in blood upon necropsy at 2 weeks after treatment with a dose of 0.5 mg kg^{-1}, 1.0 mg kg^{-1} or 1.5 mg kg^{-1} of the ABE8.8 and *PCSK9-1* LNPs. $n = 3$ monkeys per dose group; data obtained and shown in same manner as in **a**–**c**.

of tissues, we found that the liver was the predominant site of editing: we observed much lower editing in the spleen and adrenal glands, and minimal editing elsewhere (Fig. 2d). In a subsequent short-term dose–response study (using three monkeys each for doses of 0.5 mg kg^{-1}, 1.0 mg kg^{-1} and 1.5 mg kg^{-1}, with necropsy at 2 weeks), we found that all doses achieved over 50% mean base editing frequencies: *PCSK9* editing and reductions in PCSK9 and LDL cholesterol appeared to saturate at doses of ≥1.0 mg kg^{-1} (Fig. 2e–g). In both of the short-term studies, we performed liver function tests and—in some groups—noted moderate rises in aspartate aminotransferase (AST) and alanine aminotransferase (ALT) that were largely resolved by the end of the first week, and which had entirely resolved by two weeks after LNP infusion (Extended Data Fig. 5) with no adverse health events observed in any of the monkeys.

Using plasma samples taken at a range of time points up to two weeks, we measured levels of the ionizable cationic lipid and PEG-lipid components of the LNPs; both of these components were largely cleared from the circulation within two weeks (Extended Data Fig. 6a). Using additional monkeys that received a dose of 1.0 mg kg^{-1} and underwent necropsy at range of time points up to 2 weeks, we measured ABE8.8 mRNA levels in the liver and observed that they rapidly declined over the first 48 h and were nearly depleted by 1 week (Extended Data Fig. 6b).

We undertook a long-term study—which is currently ongoing, and involves four monkeys and liver biopsies taken at 2 weeks—that used a higher dose (3.0 mg kg^{-1}) to assess drug tolerability and the durability of the PCSK9 and LDL cholesterol reductions that result from *PCSK9* editing. The liver biopsy samples showed a mean 66% base editing frequency and 0.2% indel frequency (Fig. 3a). Levels of PCSK9 in the blood reached a trough by 1 week and have remained stable thereafter (up to 8 months), and have settled at a reduction of around 90% (Fig. 3b). Levels of LDL cholesterol and lipoprotein(a) in the blood have similarly achieved stable troughs that have persisted to 8 months, settling at around a 60% and around a 35% reduction, respectively (Fig. 3c, Extended Data Figs. 7, 8).

In the long-term study, there were transient and moderate rises in AST and ALT that had entirely resolved by two weeks after LNP infusion, with no changes in any other liver function tests and with no adverse health events observed to date (Extended Data Fig. 8). In a sub-study of the long-term study that included two control groups (monkeys that received phosphate-buffered saline and monkeys that received dose of 3.0 mg kg^{-1} LNPs with ABE8.8 mRNA and a non-*PCSK9* targeting gRNA) that were followed closely for 2 weeks, we observed that the increases in levels of AST and ALT were due to LNP treatment rather than *PCSK9* editing (Extended Data Fig. 9). An important issue for ongoing investigation is an adaptive immune response to the base editor: the persistence of PCSK9 and LDL cholesterol reductions for eight months with no late increases in AST and ALT demonstrates that such a response (whatever its scale) does not adversely affect the efficacy of the treatment.

Assessment of off-target editing

To evaluate off-target editing mediated by the ABE8.8 and *PCSK9-1* LNPs in primary cynomolgus monkey hepatocytes and monkey liver samples, we performed oligonucleotide enrichment and sequencing (ONE-seq)[31] using a synthetic cynomolgus monkey genomic library that was selected by homology to the *PCSK9-1* gRNA protospacer sequence, treated this library with ABE8.8 protein and *PCSK9-1* gRNA, and assessed the top 48 ONE-seq-nominated sites (of which the *PCSK9* target site was the top site) using next-generation sequencing of targeted PCR amplicons from LNP-treated versus untreated samples (Fig. 4a). In LNP-treated primary cynomolgus monkey hepatocytes, besides editing at the *PCSK9* target site there was off-target editing (mean of <1%) that was evident at only one site (designated C5), which has poor homology to the human genome (Fig. 4b, Supplementary Table 3). Assessing the same 48 sites in liver samples from monkeys that were treated with a dose of 1.0 mg kg^{-1} LNPs (from our dose–response study), we again observed off-target editing at a low level (mean of <1%) only at the C5 site (Fig. 4b, Supplementary Table 4). We discerned no off-target editing with a dose of 0.5 mg kg^{-1} LNPs, and only a low level of editing (mean <1%) with a dose of 1.5 mg kg^{-1} (Fig. 4b). The concordance of the results relating to off-target editing in primary cynomolgus monkey hepatocytes in vitro and monkey liver in vivo suggests that primary hepatocytes are an appropriate model for in vivo liver editing.

To evaluate off-target editing in primary human hepatocytes, we performed (1) ONE-seq with a synthetic human genomic library that was selected by homology to the *PCSK9-1* gRNA protospacer sequence and (2) Digenome-seq (which we adapted for use with

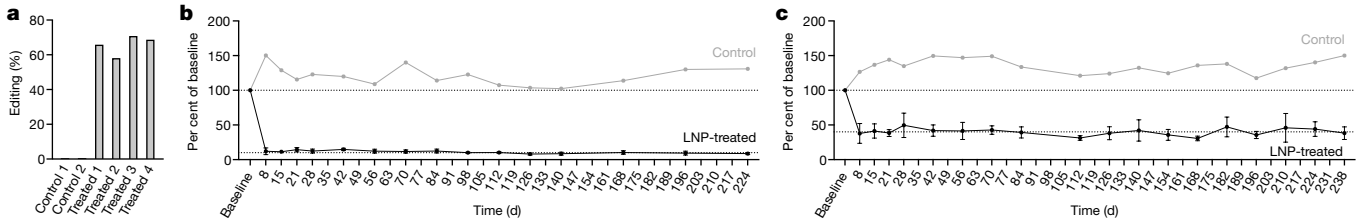

Fig. 3 | Long-term effects of adenine base editing of *PCSK9* in cynomolgus monkeys. a, Editing of the *PCSK9* exon 1 splice-donor adenine base in the livers of four cynomolgus monkeys that received an intravenous infusion of a dose of 3.0 mg kg^{-1} LNP formulation with ABE8.8 mRNA and *PCSK9-1* gRNA, and two control monkeys that received PBS. For each monkey, editing was assessed in a liver biopsy sample at two weeks after treatment. $n = 1$ sample per monkey. **b**, **c**, Changes in the levels of PCSK9 (**b**) and LDL cholesterol (**c**) in blood of the six monkeys from **a**, comparing levels at various time points up to 238 days after treatment with the baseline level before treatment. Mean ± s.d. for the LNP-treated group ($n = 4$ monkeys) and mean for the control group ($n = 2$ monkeys), at each time point. The dotted lines indicate 100% and 10% (**b**) or 100% and 40% (**c**) of baseline levels.

adenine base editors[32,33]) using whole-genome sequencing of human hepatocyte genomic DNA treated with ABE8.8 protein and *PCSK9-1* gRNA. We assessed the top 46 ONE-seq-nominated sites and the top 33 Digenome-seq-nominated sites (10 sites were common to both lists) in LNP-treated versus untreated hepatocytes from four individual donors (Fig. 4a). There was discernible editing only at the *PCSK9* target site (Fig. 4c, Supplementary Table 5).

Adenine base editors have previously been reported to induce gRNA-independent RNA editing via the deoxyadenosine deaminase domain[34,35]. We assessed for RNA editing by performing RNA sequencing of primary human hepatocytes in three states: cells treated with ABE8.8 mRNA and *PCSK9-1* gRNA; cells treated with *Streptococcus pyogenes Cas9* mRNA and *PCSK9-1* gRNA (control); and untreated cells. Comparing the RNA profiles of hepatocytes treated with ABE8.8 or *Streptococcus pyogenes* Cas9 with untreated hepatocytes, we did not observe any substantial additional RNA edits in the hepatocytes treated with ABE8.8 (Fig. 4d). The possibility remains of gRNA-independent DNA editing with adenine base editors, but we were not able to test for such editing with the standard approach of performing whole-genome sequencing of clonally expanded, editor-treated cells, owing to the current lack of a protocol for clonal expansion of single primary human hepatocytes in vitro.

Discussion

In our studies, adenine base editing proved to be highly effective in knocking down gene function in the liver of the cynomolgus monkey, achieving over 60% editing. Given that PCSK9 is largely produced by hepatocytes and that around 70% of the cells in the liver are hepatocytes, our observation of a reduction of about 90% in PCSK9 in the blood strongly suggests that we edited both *PCSK9* alleles in almost all hepatocytes in the liver. The reduction in LDL cholesterol observed in our long-term study (around 60%) surpasses or matches the effects of drugs currently used to lower LDL cholesterol—including statins, ezetimibe, bempedoic acid, lomitapide, mipomersen (an antisense oligonucleotide), PCSK9 and ANGPTL3 antibodies, and inclisiran (siRNA)—in patients. Unlike all of these drugs (which range from chronic once-daily to twice-yearly dosing), gene-editing approaches offer the potential for once-and-done therapies for the lifelong treatment of disease. Although the permanence of CRISPR-based liver editing remains to be established, in our long-term study in cynomolgus monkeys there are no signs of attenuation of the pharmacodynamic effects of liver editing over time.

We note that there are unpublished reports of the use of zinc-finger nucleases or CRISPR–Cas9 nuclease (delivered by adeno-associated viral (AAV) vectors or by LNPs) to modify various liver genes in nonhuman primates in preclinical studies and in patients in clinical trials. Although there are not yet reports of clinical efficacy for any of these treatments, neither have there been reports of serious adverse events. A previously published study has reported that AAV-delivered meganucleases targeting *PCSK9* in the liver durably reduced protein levels and LDL cholesterol in ten nonhuman primates for up to three years after treatment[36]. The findings of this study contrast with our use of base editing in cynomolgus monkeys in four ways. First, the highest level of liver editing achieved with a meganuclease was 46% in the single monkey that received the highest AAV dose (3×10^{13} genome copies per kg); at the lower AAV doses of 2×10^{12} or 6×10^{12} genome copies per kg, the mean editing levels were 12% and 26%, respectively. By contrast, we observed that the LNP-delivered base editor reproducibly achieved mean editing of over 50% in several monkeys at each of the full range of doses we tested (0.5 mg kg^{-1} to 3.0 mg kg^{-1}). Second, the use of a meganuclease to edit the gene via a double-strand break incurred a large degree of integration of the AAV vector sequence into the genome at the site of the break, with the sequence insertions being the most common editing event. Our use of a base editor resulted in the precise alteration of a single base pair as the predominant editing event and had no risk of vector sequence integration, owing to the use of mRNA rather than a DNA vector. Third, the use of an AAV vector with prolonged expression of a meganuclease elicited moderate rises in AST and ALT that appeared a few weeks after treatment and lasted for a few additional weeks to months, concomitant with a robust immune response. Our use of LNPs with brief mRNA expression of the base editor was associated with immediate mild-to-moderate rises in AST and ALT that resolved within one to two weeks and were entirely stable thereafter. Fourth, the meganucleases induced off-target editing at numerous genomic sites in the nonhuman primate liver and in human hepatocytes, whereas we discerned off-target editing at only one site in the cynomolgus monkey liver and no off-target editing in human hepatocytes.

It is premature to draw any conclusions about the relative merits of standard nuclease editing and base editing for clinical applications. Nonetheless, one advantage of base editing is its ability to efficiently and precisely introduce single-nucleotide changes in disease-associated genes in vivo, which is not straightforward to achieve with standard gene-editing nucleases owing to the inefficiency of homology-directed repair. Although standard nucleases may be as well-suited as base editors for the knockdown of genes such as *PCSK9* (owing to the efficient induction of indel mutations by non-homologous end-joining repair of double-strand breaks), the precise correction of disease-causing single-nucleotide mutations in the liver and other organs lies more squarely within the reach of base editing, as has previously been demonstrated in mouse models of genetic disorders such as phenylketonuria (through the correction of *Pah* mutations by a cytosine base editor)[37], hereditary tyrosinaemia type 1 (through the correction of *Fah* mutations by an adenine base editor)[38], and Hutchinson–Gilford progeria syndrome (through the correction of *LMNA* transgene mutations by an adenine base editor)[39].

Further evaluation of the risks of base editing in vivo is warranted before first-in-human studies. For patients for whom the risks are

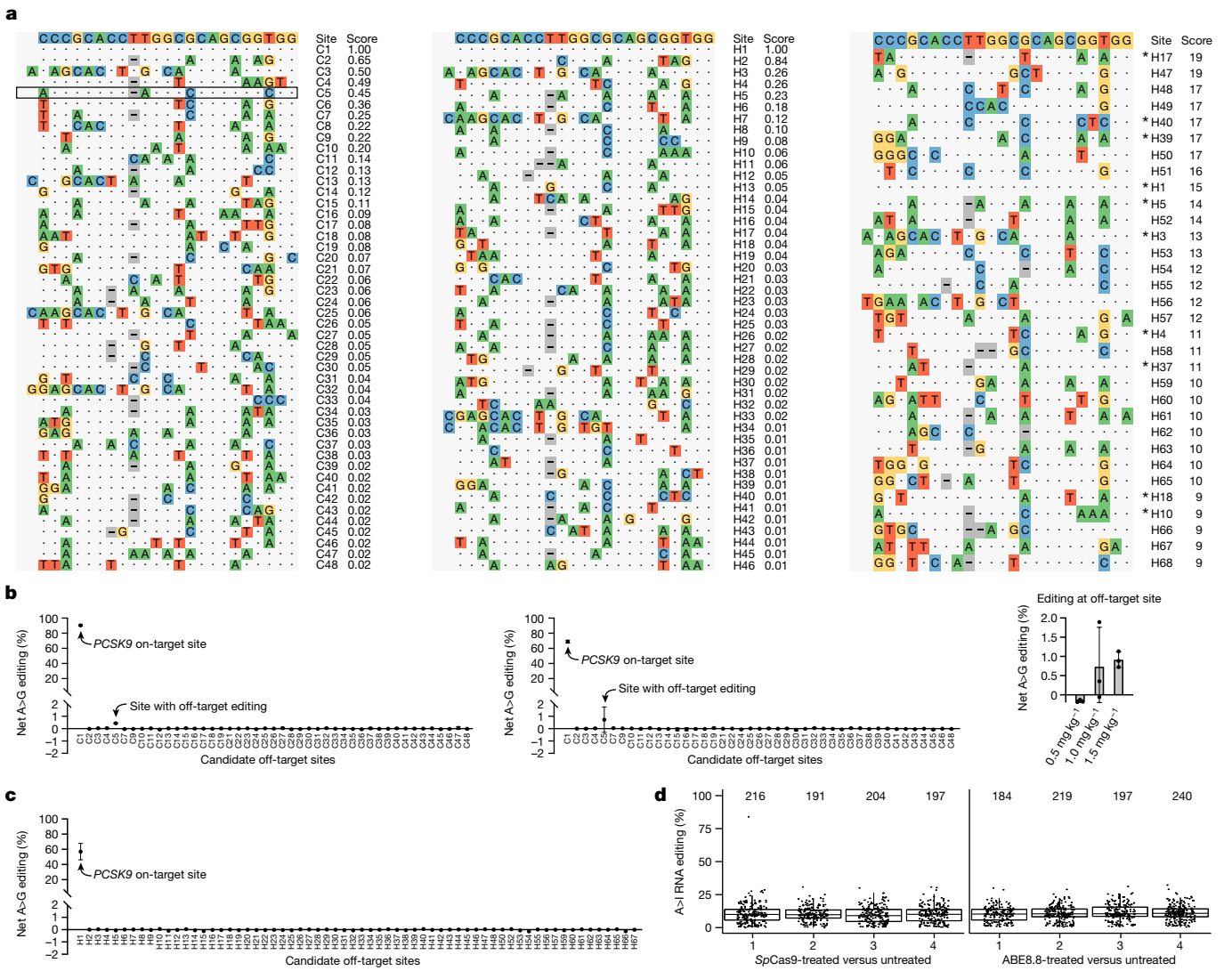

Fig. 4 | Assessment of off-target editing in primary cynomolgus monkey hepatocytes and liver, and in primary human hepatocytes. a, Candidate sites for gRNA-dependent DNA editing nominated by ONE-seq with cynomolgus monkey genomic library (left), ONE-seq with human genomic library (middle) and Digenome-seq with human hepatocyte genomic DNA (right). In the left panel, the box highlights the C5 off-target site. In the right panel, the asterisks indicate Digenome-seq-nominated sites that overlap with ONE-seq sites. **b**, gRNA-dependent DNA editing calculated as net A-to-G editing (proportion of sequencing reads with alteration of one or more adenine bases to guanine in LNP-treated samples versus untreated samples) at the on-target *PCSK9* site and the candidate off-target *PCSK9* sites in primary cynomolgus monkey hepatocytes (left) (mean ± s.d. for each site, $n = 3$ treated and 3 untreated biological replicates) and in cynomolgus monkey liver (middle and right) (mean ± s.d. for each site, $n = 3$ LNP-treated monkeys and 3 monkeys that received PBS, with each monkey represented by pooled genomic DNA from eight samples distributed throughout the liver). **c**, gRNA-dependent DNA editing in primary human hepatocytes, calculated as net A-to-G editing at the on-target *PCSK9* site and the candidate off-target *PCSK9* sites in primary human hepatocytes from four individual donors. Mean ± s.d. $n = 4$ LNP-treated and 4 untreated samples for each site. **d**, gRNA-independent RNA editing, assessed in hepatocytes treated with *Streptococcus pyogenes* Cas9 (*Sp*Cas9) or ABE8.8 after two days. $n = 4$ biological replicates. The jitter plots portray transcriptomic loci with editing in the treated sample. The number indicates the total number of edited loci that we identified in the treated sample. In the box plots, centre is median, bounds are the 25th (Q1) and 75th (Q3) percentiles, lower whisker is the maximum of (minimum editing per cent, Q1 − 1.5 × (Q3 − Q1)), and the upper whisker is the minimum of (maximum editing per cent, Q3 + 1.5 × (Q3 − Q1)), with respect to the proportion of edited reads across all edited loci in the sample.

substantially outweighed by the benefits, somatic base-editing therapies that target the liver or other organs could prove to be indispensable in addressing all manner of disease.

Online content

Any methods, additional references, Nature Research reporting summaries, source data, extended data, supplementary information, acknowledgements, peer review information; details of author contributions and competing interests; and statements of data and code availability are available at https://doi.org/10.1038/s41586-021-03534-y.

1. Jinek, M. et al. A programmable dual-RNA-guided DNA endonuclease in adaptive bacterial immunity. *Science* **337**, 816–821 (2012).
2. Zetsche, B. et al. Cpf1 is a single RNA-guided endonuclease of a class 2 CRISPR-Cas system. *Cell* **163**, 759–771 (2015).
3. Strecker, J. et al. Engineering of CRISPR–Cas12b for human genome editing. *Nat. Commun.* **10**, 212 (2019).
4. Komor, A. C., Kim, Y. B., Packer, M. S., Zuris, J. A. & Liu, D. R. Programmable editing of a target base in genomic DNA without double-stranded DNA cleavage. *Nature* **533**, 420–424 (2016).
5. Gaudelli, N. M. et al. Programmable base editing of A•T to G•C in genomic DNA without DNA cleavage. *Nature* **551**, 464–471 (2017).
6. Doudna, J. A. The promise and challenge of therapeutic genome editing. *Nature* **578**, 229–236 (2020).
7. GBD 2017 Causes of Death Collaborators. Global, regional, and national age-sex-specific mortality for 282 causes of death in 195 countries and territories, 1980-2017: a systematic analysis for the Global Burden of Disease Study 2017. *Lancet* **392**, 1736–1788 (2018).

8. Anzalone, A. V. et al. Search-and-replace genome editing without double-strand breaks or donor DNA. *Nature* **576**, 149–157 (2019).
9. Yin, H. et al. Genome editing with Cas9 in adult mice corrects a disease mutation and phenotype. *Nat. Biotechnol.* **32**, 551–553 (2014).
10. Ding, Q. et al. Permanent alteration of *PCSK9* with in vivo CRISPR-Cas9 genome editing. *Circ. Res.* **115**, 488–492 (2014).
11. Yin, H. et al. Structure-guided chemical modification of guide RNA enables potent non-viral in vivo genome editing. *Nat. Biotechnol.* **35**, 1179–1187 (2017).
12. Finn, J. D. et al. A single administration of CRISPR/Cas9 lipid nanoparticles achieves robust and persistent in vivo genome editing. *Cell Rep.* **22**, 2227–2235 (2018).
13. Chadwick, A. C., Wang, X. & Musunuru, K. In vivo base editing of *PCSK9* (proprotein convertase subtilisin/kexin type 9) as a therapeutic alternative to genome editing. *Arterioscler. Thromb. Vasc. Biol.* **37**, 1741–1747 (2017).
14. Ryu, S. M. et al. Adenine base editing in mouse embryos and an adult mouse model of Duchenne muscular dystrophy. *Nat. Biotechnol.* **36**, 536–539 (2018).
15. Rossidis, A. C. et al. In utero CRISPR-mediated therapeutic editing of metabolic genes. *Nat. Med.* **24**, 1513–1518 (2018).
16. Abifadel, M. et al. Mutations in *PCSK9* cause autosomal dominant hypercholesterolemia. *Nat. Genet.* **34**, 154–156 (2003).
17. Cohen, J. C., Boerwinkle, E., Mosley, T. H., Jr & Hobbs, H. H. Sequence variations in *PCSK9*, low LDL, and protection against coronary heart disease. *N. Engl. J. Med.* **354**, 1264–1272 (2006).
18. Rao, A. S. et al. Large-scale phenome-wide association study of *PCSK9* variants demonstrates protection against ischemic stroke. *Circ. Genom. Precis. Med.* **11**, e002162 (2018).
19. Zhao, Z. et al. Molecular characterization of loss-of-function mutations in *PCSK9* and identification of a compound heterozygote. *Am. J. Hum. Genet.* **79**, 514–523 (2006).
20. Hooper, A. J., Marais, A. D., Tanyanyiwa, D. M. & Burnett, J. R. The C679X mutation in *PCSK9* is present and lowers blood cholesterol in a southern African population. *Atherosclerosis* **193**, 445–448 (2007).
21. Ray, K. K. et al. Inclisiran in patients at high cardiovascular risk with elevated LDL cholesterol. *N. Engl. J. Med.* **376**, 1430–1440 (2017).
22. Brandts, J. & Ray, K. K. Low density lipoprotein cholesterol-lowering strategies and population health: time to move to a cumulative exposure model. *Circulation* **141**, 873–876 (2020).
23. Choudhry, N. K. et al. Full coverage for preventive medications after myocardial infarction. *N. Engl. J. Med.* **365**, 2088–2097 (2011).
24. Rodriguez, F. et al. Association of statin adherence with mortality in patients with atherosclerotic cardiovascular disease. *JAMA Cardiol.* **4**, 206–213 (2019).
25. Hines, D. M., Rane, P., Patel, J., Harrison, D. J. & Wade, R. L. Treatment patterns and patient characteristics among early initiators of PCSK9 inhibitors. *Vasc. Health Risk Manag.* **14**, 409–418 (2018).
26. Zafrir, B., Egbaria, A., Stein, N., Elis, A. & Saliba, W. PCSK9 inhibition in clinical practice: treatment patterns and attainment of lipid goals in a large health maintenance organization. *J. Clin. Lipidol.* **15**, 202–211.e2 (2021).
27. Gaudelli, N. M. et al. Directed evolution of adenine base editors with increased activity and therapeutic application. *Nat. Biotechnol.* **38**, 892–900 (2020).
28. Hendel, A. et al. Chemically modified guide RNAs enhance CRISPR–Cas genome editing in human primary cells. *Nat. Biotechnol.* **33**, 985–989 (2015).
29. Conway, A. et al. Non-viral delivery of zinc finger nuclease mRNA enables highly efficient in vivo genome editing of multiple therapeutic gene targets. *Mol. Ther.* **27**, 866–877 (2019).
30. Villiger, L. et al. In vivo cytidine base editing of hepatocytes without detectable off-target mutations in RNA and DNA. *Nat. Biomed. Eng.* **5**, 179–189 (2021).
31. Petri, K. et al. Global-scale CRISPR gene editor specificity profiling by ONE-seq identifies population-specific, variant off-target effects. Preprint at https://doi.org/10.1101/2021.04.05.438458 (2021).
32. Liang, P. et al. Genome-wide profiling of adenine base editor specificity by EndoV-seq. *Nat. Commun.* **10**, 67 (2019).
33. Kim, D., Kim, D. E., Lee, G., Cho, S. I. & Kim, J. S. Genome-wide target specificity of CRISPR RNA-guided adenine base editors. *Nat. Biotechnol.* **37**, 430–435 (2019).
34. Grünewald, J. et al. Transcriptome-wide off-target RNA editing induced by CRISPR-guided DNA base editors. *Nature* **569**, 433–437 (2019).
35. Zhou, C. et al. Off-target RNA mutation induced by DNA base editing and its elimination by mutagenesis. *Nature* **571**, 275–278 (2019).
36. Wang, L. et al. Long-term stable reduction of low-density lipoprotein in nonhuman primates following in vivo genome editing of PCSK9. *Mol. Ther.* https://doi.org/10.1016/j.ymthe.2021.02.020 (2021).
37. Villiger, L. et al. Treatment of a metabolic liver disease by in vivo genome base editing in adult mice. *Nat. Med.* **24**, 1519–1525 (2018).
38. Song, C. Q. et al. Adenine base editing in an adult mouse model of tyrosinaemia. *Nat. Biomed. Eng.* **4**, 125–130 (2020).
39. Koblan, L. W. et al. In vivo base editing rescues Hutchinson–Gilford progeria syndrome in mice. *Nature* **589**, 608–614 (2021).

Methods

No statistical methods were used to predetermine sample size. The experiments were not randomized, and investigators were not blinded to allocation during experiments and outcome assessment.

RNA production

We used 100-mer gRNAs that were chemically synthesized under solid phase synthesis conditions by commercial suppliers (Agilent, Axolabs, BioSpring, Nitto Avecia) with minimal end-modifications[28] for in vitro screening and cellular screening experiments. For example, the screening gRNA with the *PCSK9-1* protospacer sequence had the following end-modified configuration (in which lowercase lettering and asterisks indicate 2′-O-methylation and phosphorothioate linkage, respectively): 5′-c*c*c*GCACCUUGGCGCAGCGGGUUUUAGAGCUAGAAAUAGCAAGU UAAAAUAAGGCUAGUCCGUUAUCAACUUGAAAAAGUGGCACCGAGU CGGUGCU*u*u*u-3′. The corresponding highly modified gRNA having the same protospacer with heavy 2′-O-methylribosugar modification in the design was prepared at in vivo scale (100–500 mg) as previously described[12] for mouse and nonhuman primate studies.

Owing to the length of >4 kb being prohibitive for chemical synthesis, ABE8.8 or *Sp*Cas9 mRNA was produced via in vitro transcription and purification. In brief, a plasmid DNA template containing the ABE8.8-m coding sequence[27] or *Sp*Cas9 coding sequence and a 3′ polyadenylate sequence was linearized by BspQI restriction enzyme digestion. An in vitro transcription reaction containing linearized DNA template, T7 RNA polymerase, NTPs and cap analogue was performed to produce mRNA containing N^1-methylpseudouridine. After digestion of the DNA template with DNase I, the mRNA product underwent purification and buffer exchange, and the purity of the final mRNA product was assessed with capillary gel electrophoresis.

LNP formulation

For mouse studies, LNPs were formulated as previously described[12] with some modifications, and contained ABE8.8 mRNA and *PCSK9-1m* gRNA in a 1:1 ratio by weight. The LNPs had a particle size of 95–105 nm (Z-Ave, hydrodynamic diameter), with a polydispersity index of <0.1 as determined by dynamic light scattering (Malvern NanoZS Zetasizer) and 95–100% total RNA encapsulation as measured by the Quant-iT Ribogreen Assay (Thermo Fisher).

For cynomolgus monkey and cellular studies, LNPs were formulated as previously described[29,30], with the lipid components (proprietary ionizable cationic lipid, 1,2-distearoyl-*sn*-glycero-3-phosphocholine, cholesterol and a PEG-lipid) being rapidly mixed with an aqueous buffer solution containing ABE8.8 mRNA and *PCSK9-1* or non-targeting gRNA in a 1:1 ratio by weight. Ionizable cationic lipid and LNP compositions are described in patent applications WO/2017/004143A1 and WO/2017/075531A1. The resulting LNP formulations were subsequently dialysed against 1× PBS and filtered using a 0.2-μm sterile filter. The LNPs had an average hydrodynamic diameter of 55–64 nm, with a polydispersity index of <0.075 as determined by dynamic light scattering and 94–97% total RNA encapsulation as measured by the Quant-iT Ribogreen Assay.

Transfection or LNP treatment of primary hepatocytes

Primary human hepatocytes and primary cynomolgus monkey hepatocytes were obtained as frozen aliquots from BioIVT. Four lots of primary human hepatocytes—each derived from a de-identified individual donor, and designated STL, HLY, JLP and TLY—were used for the experiments: STL (main donor) was used for all experiments, including screening experiments and off-target experiments; HLY, JLP and TLY were used for off-target experiments. There were two lots of primary cynomologus monkey hepatocytes, designated HFG and UMP. The HFG lot of primary cynomolgus monkey hepatocytes was used for screening experiments, and the UMP lot was used for off-target experiments. Following the manufacturer's instructions, cells were thawed and rinsed before plating in 24-well plates that had been coated with bovine collagen overnight, with a density of about 350,000 cells per well in INVITROGRO hepatocyte medium supplemented with TORPEDO antibiotic mix (BioIVT). Four hours after plating, transfection of the cells was performed using Lipofectamine MessengerMAX Transfection Reagent (Thermo Fisher). ABE8.8 mRNA and gRNA were mixed in a 1:1 ratio by weight, diluted in Opti-MEM (Thermo Fisher), and combined with the transfection reagent diluted in Opti-MEM according to the manufacturer's instructions. The transfection mix was added directly to the growth medium in each well such that the desired dose of combined RNA was present in the well (for example, 2,500 ng ml^{-1}). The medium was not changed following transfection. For LNP-treated cells, the experiments proceeded in exactly the same way except that instead of using transfection reagent, pre-formulated LNPs were diluted in Opti-MEM and directly added to the growth medium in each well such that the desired dose of combined RNA was present in the well (for example, 2,500 ng ml^{-1}).

For experiments involving DNA analysis, the cells were removed from the plates by scraping three days after transfection or LNP treatment, washed with PBS, and collected for genomic DNA either with the DNeasy Blood & Tissue Kit (QIAGEN) or with the KingFisher Flex Purification System (Thermo Fisher) according to the manufacturer's instructions. For experiments involving RNA analysis, the cells were removed from the plates by scraping either two or three days after transfection and washed with PBS; some of the collected cells were processed with the miRNeasy Mini Kit (QIAGEN) according to the manufacturer's instructions to isolate both large and small RNA species, and the rest were collected for genomic DNA to establish *PCSK9* editing and thereby confirm base editor activity in the cells.

LNP treatment of mice

The mouse studies were approved by the Institutional Animal Care and Use Committee of the Charles River Accelerator and Development Lab (CRADL), where the studies were performed. Female C57BL/6J mice were obtained from The Jackson Laboratory and used for experiments at 8–10 weeks of age, with random assignment of mice to various experimental groups, and with collection and analysis of data performed in a blinded fashion. The sample sizes for the experimental groups were chosen in accordance with precedents in the field[37–39]. The mice were maintained on a 12-h light/12-h dark cycle, with a temperature range of 65 °F to 75 °F and a humidity range of 40% to 60%. LNPs were administered to the mice via injection into the lateral tail vein. One week following treatment, the mice were euthanized, and liver samples were obtained on necropsy and processed with the KingFisher Flex Purification System according to the manufacturer's instructions to isolate genomic DNA.

LNP treatment of cynomolgus monkeys

The cynomolgus monkey studies were approved by the Institutional Animal Care and Use Committees of Envol Biomedical and Altasciences. The pilot short-term cynomolgus monkey study was performed at Envol Biomedical, and the other cynomolgus monkey studies were performed (or, in the case of the ongoing long-term cynomolgus monkey study, is being performed) at Altasciences with the studies using male cynomolgus monkeys of Cambodian origin. The monkeys were 2–3 years of age and 2–3 kg in weight at the time of study initiation. All monkeys were genotyped at the *PCSK9* editing site to ensure that any monkeys that received the ABE8.8 and *PCSK9-1* LNPs were homozygous for the protospacer DNA sequence perfectly matching the gRNA sequence; otherwise, monkeys were randomly assigned to various experimental groups, with collection and analysis of data performed in a blinded fashion. The sample sizes for the experimental groups were chosen based on ethical principles (that is, the minimum necessary number of monkeys). The monkeys were premedicated with 1 mg kg^{-1} dexamethasone,

0.5 mg kg^{-1} famotidine and 5 mg kg^{-1} diphenhydramine on the day before LNP administration and then 30–60 min before LNP administration. The LNPs were administered via intravenous infusion into a peripheral vein over the course of 1 h. Control monkeys that received PBS instead of LNPs experienced the same infusion conditions.

For blood chemistry samples, monkeys were fasted for at least 4 h before collection via peripheral venipuncture. In all cynomolgus monkey studies, samples were typically collected on the following schedule: day −10, day −7, day −5, day 1 (6 h after LNP infusion), day 2, day 3, day 5, day 8 and day 15. In the long-term study, samples were also collected at day 21 and day 28 and have generally been collected every 2 weeks thereafter. Blood samples were analysed by the study site for LDL cholesterol, HDL cholesterol, total cholesterol, triglycerides, AST, ALT, alkaline phosphatase, γ-glutamyltransferase, total bilirubin and albumin. For each analyte, the baseline value was calculated as the mean of the values at day −10, day −7 and day −5. Some plasma samples were sent to Charles River Laboratories for analysis for levels of the ionizable cationic lipid and PEG-lipid components of the LNPs. A portion of each blood sample was sent to the investigators for PCSK9 measurement using the LEGEND MAX Human PCSK9 ELISA Kit (BioLegend), with recombinant cynomolgus monkey PCSK9 (PC9-C5223, Acro) for standardization, or for lipoprotein(a) measurement using the lipoprotein(a) ELISA kit (Mercodia), according to the manufacturer's instructions.

In the long-term cynomolgus monkey study, each monkey underwent an ultrasonography-guided percutaneous liver biopsy using a 16-gauge biopsy needle, performed under general anaesthesia, on day 15. In the short-term cynomolgus monkey studies, each monkey underwent euthanasia and necropsy on day 15 or another time point within the first 2 weeks. Samples were collected from a variety of organs, frozen and shipped to the investigators for further analysis. For the liver, two samples each were collected from the left, middle, right and caudate lobes, for a total of eight samples per liver. Organ samples were processed with the KingFisher Flex Purification System according to the manufacturer's instructions to isolate genomic DNA.

Quantification of DNA base editing

Potential off-target sites were identified using ONE-seq and Digenome-seq, as described in 'ONE-seq' and 'Digenome-seq'. To assess for on-target and off-target editing, PCR reactions with Accuprime GC Rich DNA Polymerase (Thermo Fisher) used primers specific to the target genomic sites—designed with Primer3 v.4.1.0 (https://primer3.ut.ee/)—with 5′ Nextera adaptor sequences (Supplementary Table 6), followed by purification of the PCR amplicons with the Sequalprep Normalization Plate Kit (Thermo Fisher). A second round of PCR with the Nextera XT Index Kit V2 Set A and/or Nextera XT Index Kit V2 Set D (Illumina), followed by purification with the Sequalprep Normalization Plate Kit, generated barcoded libraries, which were pooled and quantified using a Qubit 3.0 Fluorometer. After denaturation, dilution to 10 pM, and supplementation with 15% PhiX, the pooled libraries underwent paired-end sequencing on an Illumina MiSeq System.

The amplicon sequencing data were analysed with CRISPResso2 v.2.0.31 in batch mode (CRISPRessoBatch)[40], with parameters '--default_min_aln_score 95 --quantification_window_center -10 --quantification_window_size 10 --base_editor_output --conversion_nuc_from A --conversion_nuc_to G --min_frequency_alleles_around_cut_to_plot 0.1 --max_rows_alleles_around_cut_to_plot 100'. Moreover, the parameter '--max_paired_end_reads_overlap' was set to $2R - F + 0.25 \times F$, following FLASH recommendations (http://ccb.jhu.edu/software/FLASH/)[41], in which R is the read length and F is the amplicon length. For cynomolgus monkey samples, an additional parameter '--min_single_bp_quality 30' was used. Editing was quantified from the 'Quantification_window_nucleotide_percentage_table.txt' output table as the percentage of reads that supported any A-to-G/C/T substitution in the main edited position (position 6 of the protospacer DNA sequence). For candidate off-target sites, A-to-G editing was quantified throughout the editing window (positions 1 to 10 of the protospacer DNA sequence). Indels were quantified from the 'Alleles_frequency_table_around_sgRNA_*.txt' output table as the percentage of reads that supported insertions or deletions over a 5-bp window on either side of the nick site (at position −3 upstream of the PAM sequence), having excluded reads that supported deletions larger than 30 bp.

In some cases, PCR amplicons were subjected to confirmatory Sanger sequencing, performed by GENEWIZ, with base editing frequencies estimated from the chromatograms. MIT specificity scores for gRNAs were determined using CRISPOR v.4.98 (http://crispor.tefor.net/)[42].

Quantification of RNA base editing

To assess for gRNA-independent RNA editing, primary human hepatocytes were treated with ABE8.8 mRNA and *PCSK9-1* gRNA ($n = 4$ biological replicates), were treated with Sp*Cas9* mRNA and gRNA ($n = 4$), or were untreated ($n = 4$). RNA was extracted after 2 days as described in 'Transfection or LNP treatment of primary hepatocytes'. The RNA samples were processed and sequenced by GENEWIZ; following rRNA depletion, libraries were prepared and underwent 2×150-bp paired-end sequencing on an Illumina HiSeq System, with about 50 million reads per sample. RNA-sequencing variant calling for all samples was executed using GATK Best Practices[43]. In brief, reads were aligned using STAR v.2.7.1a[44] to the GRCh38 reference genome (ftp.ncbi.nlm.nih.gov/genomes/all/GCA/000/001/405/GCA_000001405.15_GRCh38/seqs_for_alignment_pipelines.ucsc_ids/GCA_000001405.15_GRCh38_no_alt_analysis_set.fna.gz) with Gencode v.34 (ftp://ftp.ebi.ac.uk/pub/databases/gencode/Gencode_human/release_34/gencode.v34.primary_assembly.annotation.gtf.gz). We removed PCR duplicates using GATK MarkDuplicates, followed by variant identification using GATK HaplotypeCaller. Variants were then filtered by excluding those with quality of depth < 2.0 and FisherStrand (evidence of strand bias) > 30. All GATK analyses were performed with gatk4 v.4.1.8.1.

Variants obtained were further filtered by comparison with untreated control samples as follows. (1) Nucleotide distributions at each identified variant in treated cells were determined in each untreated control sample and each treated sample using perbase v.0.5.1 (https://github.com/sstadick/perbase). (2) For all variants covered by at least 20 reads in both treated and untreated conditions, RNA edits were identified as those that had the reference allele (A or T) in at least 95% of reads in all untreated control samples and the alternate allele (G or C) in at least one read in the treated sample. The above steps were executed with each of the ABE8.8-treated and *Sp*Cas9-treated samples.

To determine relative *PCSK9* expression levels in ABE8.8 and *PCSK9-1*-treated cells versus control cells, read counts per gene were obtained using STAR v.2.7.1a with option '--quantMode GeneCounts' and transcriptome annotations from Gencode v.34. Differential expression analysis was done in R v.3.6.2 (https://cran.r-project.org/) with DESeq2 v.1.26.0[45], using the condition (treated or control) as contrast. Four replicates per condition were considered.

Quantification of alternative splicing

To assess for aberrant splicing events resulting from editing of the *PCSK9* exon 1 splice-donor adenine base, primary human hepatocytes were treated with ABE8.8 mRNA and *PCSK9-1* gRNA, and RNA was extracted after 3 days as described in 'Transfection or LNP treatment of primary hepatocytes'. Reverse transcription was performed using the iScript Reverse Transcription Supermix reagent (Bio-Rad) according to the manufacturer's instructions, with four different primer pairs (Supplementary Table 6) used for PCR amplification of transcripts spanning exon 1 and exon 2, with or without any portions of intron 1. Paired-end reads of 250-bp length generated using an Illumina MiSeq System, as described in 'Quantification of DNA base editing', were trimmed for adapters using trimmomatic v.0.39[46] with parameters 'ILLUMINACLIP:NexteraPE-PE.fa:2:30:10:1:true LEADING:3 TRAILING:3 SLIDINGWINDOW:4:15 MINLEN:36'. Reads were then merged

with FLASH v.1.2.11[41] and aligned to the *PCSK9* gene body with Bowtie2 v.2.4.1[47] with parameters '--local --very-sensitive-local -k 1 --np 0'. Gene annotations were obtained from Ensembl v.98 (ftp://ftp.ensembl.org/pub/release-98/gtf/homo_sapiens/Homo_sapiens.GRCh38.98.gtf.gz). Alignments were filtered with samtools v.1.10[48] and converted to BED format with the bedtools v.2.25.0 bamtobed function[49]. We required a minimum of 1,000 mapped reads per sample and tallied the end positions of mapped reads. We report positions throughout *PCSK9* intron 1 supported by a minimum of 10 reads in at least one treated sample (Supplementary Table 2).

Quantification of ABE8.8 mRNA levels in cynomolgus monkey liver

Liver tissue samples were homogenized using Tissue & Cell Lysis Solution (Lucigen) supplemented with 1 mg ml^{-1} Proteinase K (Invitrogen), and diluted lysate was subjected to reverse transcription and PCR using the EXPRESS One-Step Superscript qRT–PCR Kit (Thermo Fisher) according to the manufacturer's instructions, with a custom primer–probe mix specific for the 3′ untranslated region of the ABE8.8 mRNA, on a CFX96 Real-Time PCR Detection System. Purified ABE8.8 mRNA was used for standardization.

Digenome-seq

Digenome-seq was adapted from previously described procedures[32,33]. Genomic DNA from primary human hepatocytes (the HLY lot) was purified using the DNeasy Blood & Tissue Kit (QIAGEN). First, ribonucleoproteins (RNPs) were prepared by combining 300 nM recombinant ABE8.8-m protein (Beam Therapeutics) with 600 nM *PCSK9-1* gRNA in 1× CutSmart Buffer (NEB) and 5% glycerol. After incubating at 25 °C for 10 min, 2 μg of genomic DNA was added to either the RNPs or a mock sample containing only buffer and glycerol. These reactions were incubated at 37 °C for 8 h. RNase A (New England Biolabs) then Proteinase K (New England Biolabs) were added in sequential steps and incubated at 37 °C to quench the reaction. Agencourt AMPure XP beads (Beckman Coulter) were used at 1.5× to purify the reactions. Both genomic DNA samples were then treated with 20 U of EndoV (New England Biolabs) at 37 °C for 1 h. After a further 1.5× AMPure XP bead purification, a quantitative PCR assay using Power SYBR Green Master Mix (Applied Biosystems) was performed to determine the cleavage efficiency of the RNP-treated sample relative to the mock control at the on-target *PCSK9* site. Following confirmation of high on-target activity, the genomic DNA of both samples was sheared using a Covaris M220 focused ultrasonicator to a target size of 300 bp (75 W peak incident power, 10% duty factor, 200 cycles per burst, for 100 s). Library preparation of these samples was performed using the NEBNext Ultra II DNA Library Prep Kit for Illumina (New England Biolabs). After end-repair and adaptor-ligation, AMPure XP bead size selection (0.6×, then 0.2×) was performed to remove larger DNA molecules before PCR amplification. Four PCR reactions were performed with each sample, using 10 ng of input DNA and 6 PCR cycles, after which each reaction was purified using 0.9× AMPure XP beads. The four samples of each condition were then combined into a single sample. Size selection of the final library samples was performed on a PippinHT system (Sage Sciences) to isolate DNA of 150–350 bp on a 3% agarose gel cassette. A final 2× AMPure XP bead purification was performed to concentrate the samples and elute in UltraPure DNase/RNase-free Distilled Water (Invitrogen). The samples underwent Illumina HiSeq 2×150-bp sequencing at 30× depth, performed by GENEWIZ.

Reads were aligned using Bowtie2 v.2.4.1 to GRCh38. Uniquely aligned reads were then processed as follows: (1) all loci in the genome that had read starts ≥ 9 in the ABE8.8-treated sample on either strand were identified as putative *Streptococcus pyogenes* nickase Cas9 nick sites (the number of read starts was used as the score); (2) for each locus identified in step 1, corresponding read-start pileups with ≥ 2 read starts on the opposite strand, that were also within a window of 4 to 13 bases from the loci (corresponding to an editing window of positions 2 to 11 in the protospacer sequence) were then identified as putative EndoV nick sites associated with the *Streptococcus pyogenes* nickase Cas9 nick sites; and (3) sites identified by the same process in the mock control sample within a window of 50 bases on either side of loci identified in the ABE8.8-treated samples were removed from further analysis. Sites that were not in chromosomes 1–22, X or Y were also removed.

ONE-seq

ONE-seq was performed as previously described[31]. The human ONE-seq library for the *PCSK9-1* gRNA was designed using the GRCh38 Ensembl v98 reference genome (ftp://ftp.ensembl.org/pub/release-98/fasta/homo_sapiens/dna/Homo_sapiens.GRCh38.dna.chromosome.{1-22,X,Y,MT}.fa and ftp://ftp.ensembl.org/pub/release-98/fasta/homo_sapiens/dna/Homo_sapiens.GRCh38.dna.nonchromosomal.fa), and the cynomolgus monkey ONE-seq library for the *PCSK9-1* gRNA was designed using the macFas5 Ensembl v.98 reference genome (ftp://ftp.ensembl.org/pub/release-98/fasta/macaca_fascicularis/dna/Macaca_fascicularis.Macaca_fascicularis_5.0.dna.chromosome.{1-20,X,MT}.fa.gz and ftp://ftp.ensembl.org/pub/release-98/fasta/macaca_fascicularis/dna/Macaca_fascicularis.Macaca_fascicularis_5.0.dna.nonchromosomal.fa.gz). Sites with up to six mismatches and sites with up to four mismatches plus up to two DNA or RNA bulges, compared to the on-target *PCSK9* site, were identified with Cas-Designer v.1.2[50]. The final oligonucleotide sequences were generated with a script[31], and the oligonucleotide libraries were synthesized by Agilent Technologies.

Duplicate ONE-seq experiments were performed with the human ONE-seq library, and a single ONE-seq experiment for the cynomolgus monkey library. Each library was PCR-amplified and subjected to 1.25× AMPure XP bead purification. After incubation at 25 °C for 10 min in CutSmart buffer, RNP comprising 769 nM recombinant ABE8.8-m protein and 1.54 μM *PCSK9-1* gRNA was mixed with 100 ng of the purified library and incubated at 37 °C for 8 h. Proteinase K was added to quench the reaction at 37 °C for 45 min, followed by 2× AMPure XP bead purification. The reaction was then serially incubated with EndoV at 37 °C for 30 min, Klenow Fragment (New England Biolabs) at 37 °C for 30 min, and NEBNext Ultra II End Prep Enzyme Mix (New England Biolabs) at 20 °C for 30 min followed by 65 °C for 30 min, with 2× AMPure XP bead purification after each incubation. The reaction was ligated with an annealed adaptor oligonucleotide duplex at 20 °C for 1 h to facilitate PCR amplification of the cleaved library products, followed by 2× AMPure XP bead purification. Size selection of the ligated reaction was performed on a PippinHT system to isolate DNA of 150–200 bp on a 3% agarose gel cassette, followed by two rounds of PCR amplification to generate a barcoded library, which underwent paired-end sequencing on an Illumina MiSeq System as described in 'Quantification of DNA base editing'.

The analysis pipeline[31] used for processing the data assigned a score quantifying the editing efficiency with respect to the on-target *PCSK9* site to each potential off-target site. Sites were ranked on the basis of this ONE-seq score, and the top sites were selected for validation; for the human library, the mean ONE-seq score between the duplicate experiments was used for site prioritization. We performed validation experiments with the top 46 human ONE-seq sites, on the basis of a cut-off ONE-seq score of 0.01; we undertook validation of the top 48 cynomolgus monkey ONE-seq sites as a comparable number to the human list.

Data analysis

Sequencing data were analysed as described above. Other data were collected and analysed using GraphPad Prism v.8.4.3.

Reporting summary

Further information on research design is available in the Nature Research Reporting Summary linked to this paper.

Data availability

DNA and RNA sequencing data that support the findings of this study have been deposited in the NCBI Sequence Read Archive with the accession code PRJNA716270. All other data supporting the findings of this study (Figs. 1–4, Extended Data Figs. 1–9) are available within the Article and its Supplementary Information. The GRCh38 reference human genome (ftp.ncbi.nlm.nih.gov/genomes/all/GCA/000/001/405/GCA_000001405.15_GRCh38/seqs_for_alignment_pipelines.ucsc_ids/GCA_000001405.15_GRCh38_no_alt_analysis_set.fna.gz, ftp://ftp.ensembl.org/pub/release-98/fasta/homo_sapiens/dna/Homo_sapiens.GRCh38.dna.chromosome.{1-22,X,Y,MT}.fa and ftp://ftp.ensembl.org/pub/release-98/fasta/homo_sapiens/dna/Homo_sapiens.GRCh38.dna.nonchromosomal.fa) and Gencode v.34 (ftp://ftp.ebi.ac.uk/pub/databases/gencode/Gencode_human/release_34/gencode.v34.primary_assembly.annotation.gtf.gz) and Ensembl v.98 (ftp://ftp.ensembl.org/pub/release-98/gtf/homo_sapiens/Homo_sapiens.GRCh38.98.gtf.gz) annotations were used. The macFas5 cynomolgus monkey reference genome (ftp://ftp.ensembl.org/pub/release-98/fasta/macaca_fascicularis/dna/Macaca_fascicularis.Macaca_fascicularis_5.0.dna.chromosome.{1-20,X,MT}.fa.gz and ftp://ftp.ensembl.org/pub/release-98/fasta/macaca_fascicularis/dna/Macaca_fascicularis.Macaca_fascicularis_5.0.dna.nonchromosomal.fa.gz) was used. Source data are provided with this paper.

Code availability

Custom codes used to analyse Digenome-seq data are provided in the Supplementary Information (files named digenome_step1.sh and digenome_step2.R), as are instructions (file named README.txt).

40. Clement, K. et al. CRISPResso2 provides accurate and rapid genome editing sequence analysis. *Nat. Biotechnol*. **37**, 224–226 (2019).
41. Magoč, T. & Salzberg, S. L. FLASH: fast length adjustment of short reads to improve genome assemblies. *Bioinformatics* **27**, 2957–2963 (2011).
42. Concordet, J. P. & Haeussler, M. CRISPOR: intuitive guide selection for CRISPR/Cas9 genome editing experiments and screens. *Nucleic Acids Res*. **46**, W242–W245 (2018).
43. Van der Auwera, G. A. et al. From FastQ data to high confidence variant calls: the Genome Analysis Toolkit best practices pipeline. *Curr. Protoc. Bioinformatics* **43**, 11.10.1–11.10.33 (2013).
44. Dobin, A. et al. STAR: ultrafast universal RNA-seq aligner. *Bioinformatics* **29**, 15–21 (2013).
45. Love, M. I., Huber, W. & Anders, S. Moderated estimation of fold change and dispersion for RNA-seq data with DESeq2. *Genome Biol*. **15**, 550 (2014).
46. Bolger, A. M., Lohse, M. & Usadel, B. Trimmomatic: a flexible trimmer for Illumina sequence data. *Bioinformatics* **30**, 2114–2120 (2014).
47. Langmead, B. & Salzberg, S. L. Fast gapped-read alignment with Bowtie 2. *Nat. Methods* **9**, 357–359 (2012).
48. Li, H. et al. The Sequence Alignment/Map format and SAMtools. *Bioinformatics* **25**, 2078–2079 (2009).
49. Quinlan, A. R. & Hall, I. M. BEDTools: a flexible suite of utilities for comparing genomic features. *Bioinformatics* **26**, 841–842 (2010).
50. Bae, S., Park, J. & Kim, J. S. Cas-OFFinder: a fast and versatile algorithm that searches for potential off-target sites of Cas9 RNA-guided endonucleases. *Bioinformatics* **30**, 1473–1475 (2014).

Acknowledgements Conception and design of the work was performed and supported by Verve Therapeutics. Acquisition, analysis and interpretation of the data was performed and supported by Verve Therapeutics, with some aspects being performed on behalf or at the direction of Verve Therapeutics. Acuitas Therapeutics supported the work by providing Verve Therapeutics with LNP reagents and manufacturing the LNP formulations. Beam Therapeutics supported the work by developing the ABE8.8-m protein sequence. We are grateful to J. K. Joung for critical reading of the manuscript.

Author contributions A.C.C. and K.G.R. conceived, designed and directed the gRNA design and screening. A.C.C. conceived, designed and directed the cell-based studies and off-target analyses. E.R. conceived, designed and directed the mouse and cynomolgus studies with design input from P.M. C.J.C. and C.W.R. conceived, designed and directed mRNA modification and codon optimization. C.J.C, K.B., C.W.R, A.S. and K.W. conceived, designed and/or directed mRNA processing optimization. K.M., A.C.C., T.M., J.E.D., C.W.R., K.W., C.D., V.C., M.A., A.B., K.B., S.B., M.C.B., H.-M.C., T.V.C., J.D.G., S.A.G., R.G., L.N.K., J.L., J.A.M., Y.M., A.M.M., Y.S.N., J.N., H.R., A.S., M.S., M.R.S., L.E.S., K.G.R., P.M., C.J.C. and E.R. contributed to wet laboratory experiments. K.M., S.P.G. and S.I. contributed to bioinformatic analyses. S.H.Y.F. and Y.K.T. contributed to the formulation and manufacture of LNPs. N.M.G. and G.C. contributed to the development of base-editing technology and specifically the ABE8.8-m protein sequence. K.M. wrote the manuscript, and all authors contributed to the editing of the manuscript. A.M.B. supervised the work with oversight by S.K. and advisory input from K.M.

Competing interests K.M. is an advisor to and holds equity in Verve Therapeutics and Variant Bio. A.M.B. is an employee of Verve Therapeutics and holds equity in Verve Therapeutics, Lyndra Therapeutics, Corner Therapeutics and Cocoon Biotech. S.K. is an employee of Verve Therapeutics, holds equity in Verve Therapeutics and Maze Therapeutics, and has served as a consultant for Acceleron, Eli Lilly, Novartis, Merck, Novo Nordisk, Novo Ventures, Ionis, Alnylam, Aegerion, Haug Partners, Noble Insights, Leerink Partners, Bayer Healthcare, Illumina, Color Genomics, MedGenome, Quest and Medscape. S.H.Y.F. and Y.K.T. are employees of and hold equity in Acuitas Therapeutics. N.M.G. and G.C. are employees of and hold equity in Beam Therapeutics. All other authors are employees of and hold equity in Verve Therapeutics. Verve Therapeutics has filed for patent protection related to various aspects of therapeutic base editing of *PCSK9*, with A.C.C., C.J.C., C.W.R., K.G.R. and E.R. as the inventors.

Additional information
Supplementary information The online version contains supplementary material available at https://doi.org/10.1038/s41586-021-03534-y.
Correspondence and requests for materials should be addressed to S.K.
Peer review information *Nature* thanks Kathryn Moore, Alan Tall, Fyodor Urnov and the other, anonymous, reviewer(s) for their contribution to the peer review of this work.
Reprints and permissions information is available at http://www.nature.com/reprints.

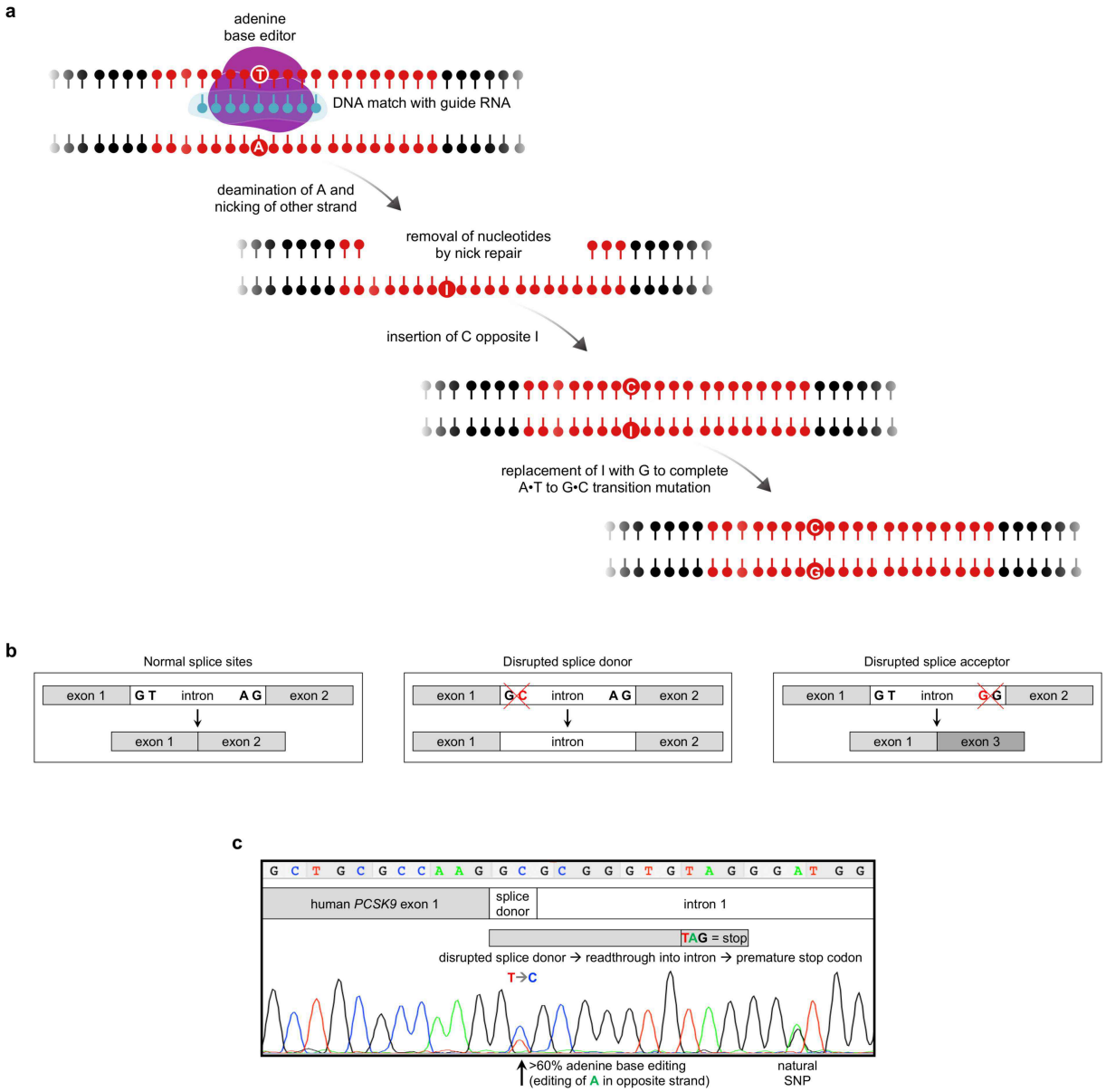

Extended Data Fig. 1 | Overview of base-editing approach. a, Schematic of adenine base editing. **b**, Schematic showing potential splicing outcomes with disruption of splice donor or splice acceptor sequences. Other outcomes are possible, such as inclusion of part of the intron in the splicing product. **c**, Schematic with Sanger sequencing chromatogram, demonstrating editing of adenine base in the antisense strand at the splice donor at the end of *PCSK9* exon 1 (PCR amplification from the genomic DNA of the cells transfected with a dose of 2,500 ng ml^{-1} in Fig. 1b), portraying how splice-site disruption results in an in-frame stop codon. Heterozygosity for a naturally occurring single-nucleotide polymorphism (SNP) is evident downstream of the editing site.

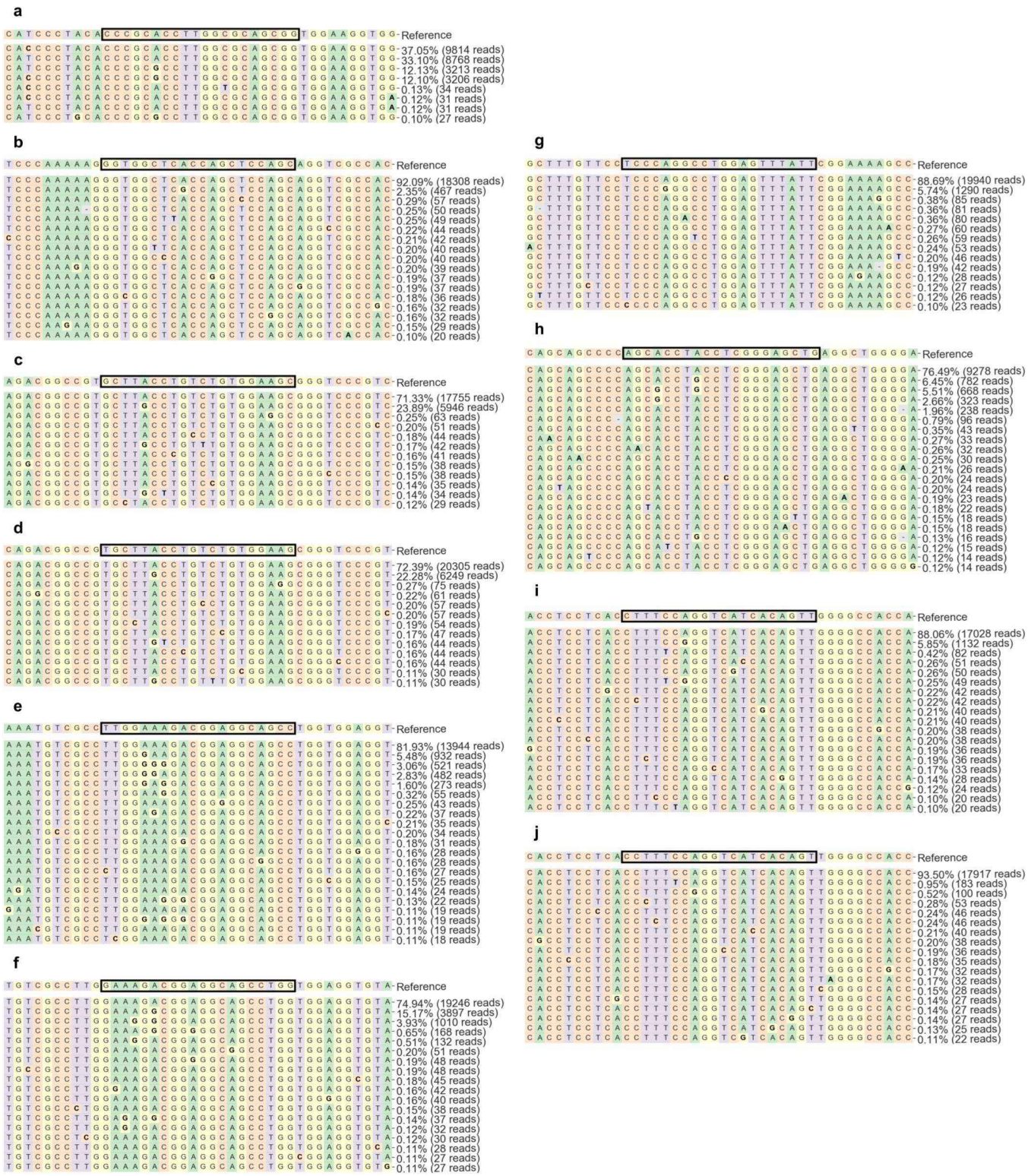

Extended Data Fig. 2 | Editing of splice-site adenine bases throughout the human *PCSK9* gene with first set of ten candidate gRNAs. Primary human hepatocytes were transfected at a dose of 5,000 ng RNA per ml; the boldface underlined letter in each of the following protospacer/PAM sequences (in which the solidus indicates the division between the protospacer and PAM) indicates the target splice-site adenine base. The black box in each panel indicates the gRNA protospacer sequence. All panels were generated with CRISPResso2. **a**, *PCSK9-1*, CCCGC**A**CCTTGGCGCAGCGG/TGG. **b**, *PCSK9-2*, GGTGGCTC**A**CCAGCTCCAGC/AGG. **c**, *PCSK9-3*, GCTT**A**CCTGTCTGTGGAAGC/GGG. **d**, *PCSK9-4*, TGCTT**A**CCTGTCTGTGGAAG/CGG. **e**, *PCSK9-5*, TTGGAA**A**GACGGAGGCAGCC/TGG. **f**, *PCSK9-6*, GAA**A**GACGGAGGCAGCCTGG/TGG. **g**, *PCSK9-7*, TCCC**A**GGCCTGGAGTTTATT/CGG. **h**, *PCSK9-8*, AGCACCT**A**CCTC GGGAGCTG/AGG. **i**, *PCSK9-9*, CTTTCC**A**GGTCATCACAGTT/GGG. **j**, *PCSK9-10*, CCTTTCC**A**GGTCATCACAGT/TGG.

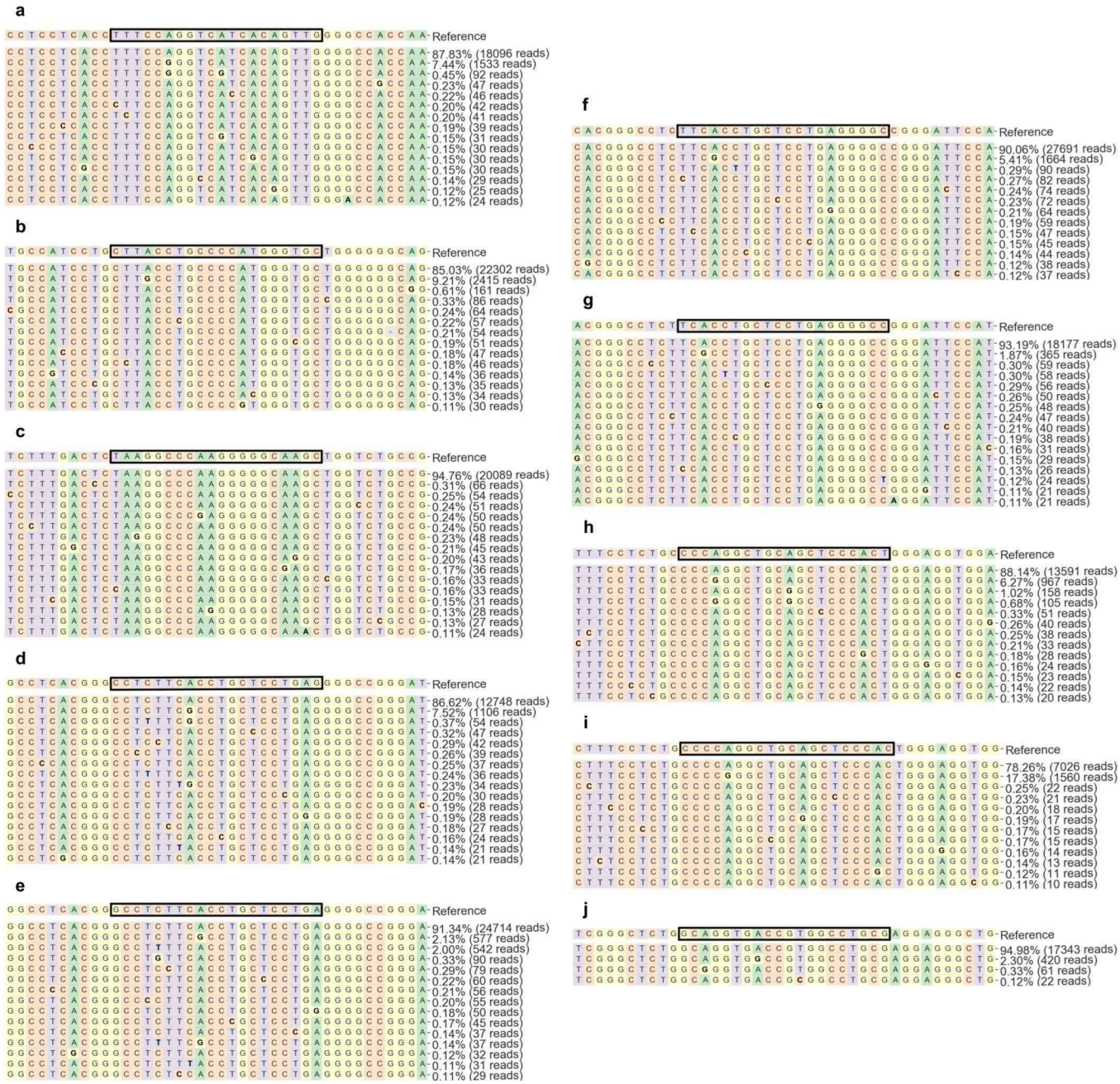

Extended Data Fig. 3 | Editing of splice-site adenine bases throughout the human *PCSK9* gene with second set of ten candidate gRNAs. Primary human hepatocytes were transfected at a dose of 5,000 ng RNA per ml; the boldface underlined letter in each of the following protospacer/PAM sequences (in which the solidus indicates the division between the protospacer and PAM) indicates the target splice-site adenine base. The black box in each panel indicates the gRNA protospacer sequence. All panels were generated with CRISPResso2. **a**, *PCSK9-11*, TTTCC**A**GGTCATCACAGTTG/GGG. **b**, *PCSK9-12*, CTT**A**CCTGCCCCATGGGTGC/TGG. **c**, *PCSK9-13*, TA**A**GGCCCAAGGGGGCAAGC/TGG. **d**, *PCSK9-14*, CCTCTTC**A**CCTGCTCCTGAG/GGG. **e**, *PCSK9-15*, GCCTCT TC**A**CCTGCTCCTGA/GGG. **f**, *PCSK9-16*, TTC**A**CCTGCTCCTGAGGGGC/CGG. **g**, *PCSK9-17*, TC**A**CCTGCTCCTGAGGGGCC/GGG. **h**, *PCSK9-18*, CCC**A**GGCTGC AGCTCCCACT/GGG. **i**, *PCSK9-19*, CCCC**A**GGCTGCAGCTCCCAC/TGG. **j**, *PCSK9-20*, GC**A**GGTGACCGTGGCCTGCG/AGG.

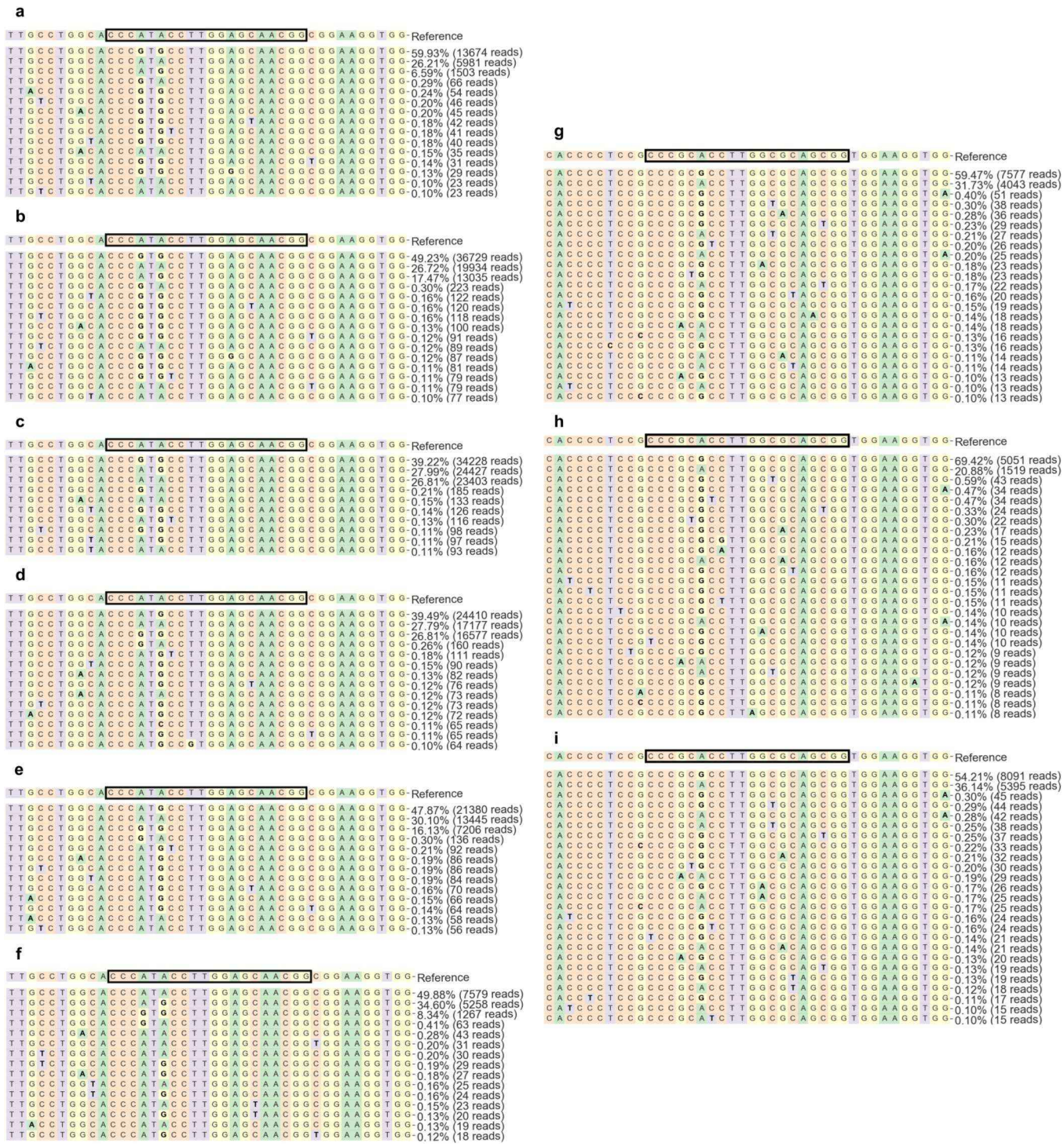

Extended Data Fig. 4 | Editing of *PCSK9* exon 1 splice-donor adenine base in mice and in cynomolgus monkeys. a–f, Representative liver samples from mice treated with LNPs with *PCSK9-1m* gRNA (portrayed in Fig. 1e). Protospacer/PAM sequence, CCCAT**A**CCTTGGAGCAACGG/CGG (in which the solidus indicates the division between the protospacer and PAM, and the boldface underlined letter indicates the target splice-donor adenine base). The black box in each panel indicates the gRNA protospacer sequence. All panels were generated with CRISPResso2. LNP doses were 2.0 mg kg^{-1} (**a**), 1.0 mg kg^{-1} (**b**), 0.5 mg kg^{-1} (**c**), 0.25 mg kg^{-1} (**d**), 0.125 mg kg^{-1} (**e**) and 0.05 mg kg^{-1} (**f**). **g–i**, Representative liver samples from three monkeys treated with a dose of 1.0 mg kg^{-1} of LNPs with *PCSK9-1* gRNA, portrayed in Fig. 2a–d (treated monkeys 1, 2 and 3). Protospacer/PAM sequence, CCCGC**A**CCTTGGCGCAGCGG/TGG (in which the solidus indicates the division between the protospacer and PAM, and the boldface underlined letter indicates the target splice-donor adenine base). The black box in each panel indicates the gRNA protospacer sequence. All panels were generated with CRISPResso2.

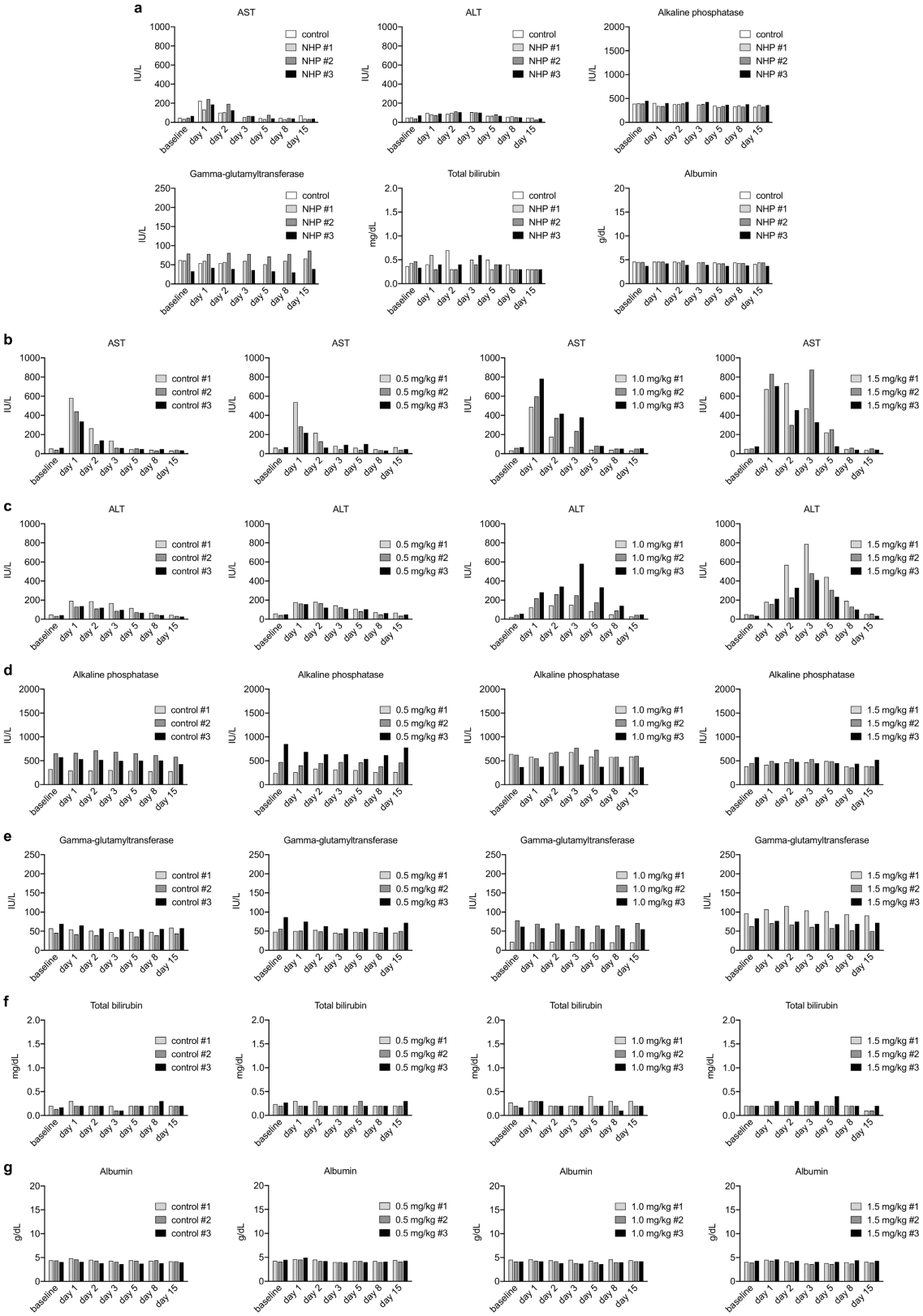

Extended Data Fig. 5 | Liver function tests in short-term cynomolgus monkey studies. a, Absolute values of blood levels of AST, ALT, alkaline phosphatase, γ-glutamyltransferase, total bilirubin and albumin in the three LNP-treated monkeys in Fig. 2a–d, as well as a contemporaneous control monkey that received PBS, at various time points up to 15 days. $n = 1$ blood sample per monkey at each time point. Some values are missing for the control monkey (all day 3 values, all later γ-glutamyltransferase values). **b**–**g**, Absolute values of blood levels of AST (**b**), ALT (**c**), alkaline phosphatase (**d**), γ-glutamyltransferase (**e**), total bilirubin (**f**) and albumin (**g**) in the individual monkeys portrayed in Fig. 2e–g, as well as in non-contemporaneous control monkeys that received PBS, at various time points up to 15 days. $n = 1$ blood sample per monkey at each time point.

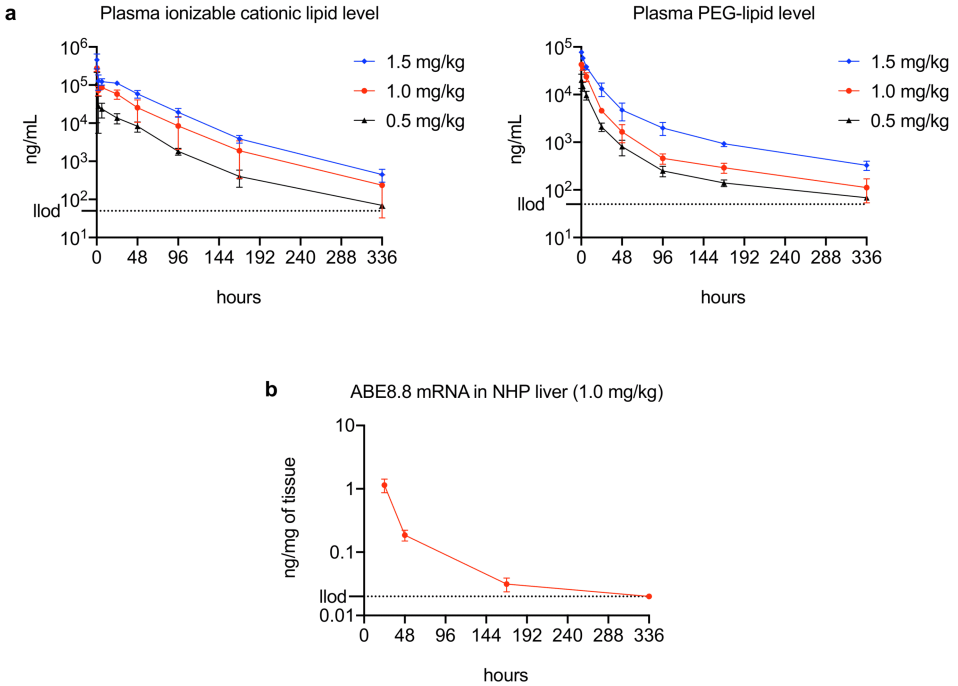

Extended Data Fig. 6 | Pharmacokinetics of ABE8.8 and *PCSK9-1* LNPs in cynomolgus monkeys. a, Plasma levels of ionizable cationic lipid and PEG-lipid components of ABE8.8 and *PCSK9-1* LNPs at various LNP doses in the monkeys portrayed in Fig. 2e–g (mean ± s.d. for each group, $n = 3$ monkeys per dose group) at various time points up to 2 weeks after treatment. llod, lower limit of detection. **b**, Liver ABE8.8 mRNA levels in monkeys that received a dose of 1.0 mg kg^{-1} LNPs (mean ± s.d. for each group, $n = 4$ monkeys per necropsy group) at various time points up to 2 weeks after treatment.

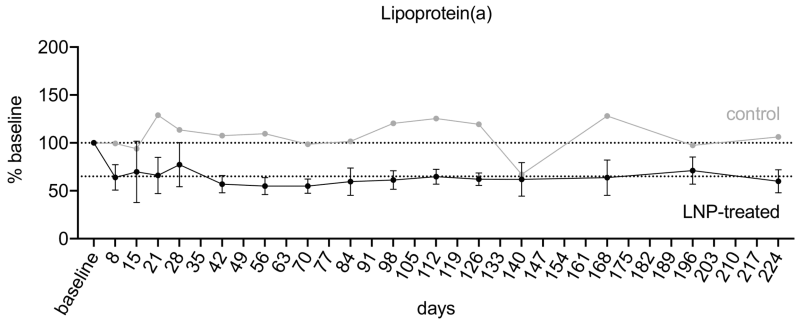

Extended Data Fig. 7 | Long-term effects of adenine base editing of *PCSK9* on lipoprotein(a) in cynomolgus monkeys. Changes in the blood lipoprotein(a) level in the six monkeys from Fig. 3a, comparing levels at various time points up to 238 days after treatment versus the baseline level before treatment. Mean ± s.d. for the LNP-treated group ($n = 4$ monkeys) and mean for the control group ($n = 2$ monkeys) at each time point). The dotted lines indicate 100% and 65% of baseline levels.

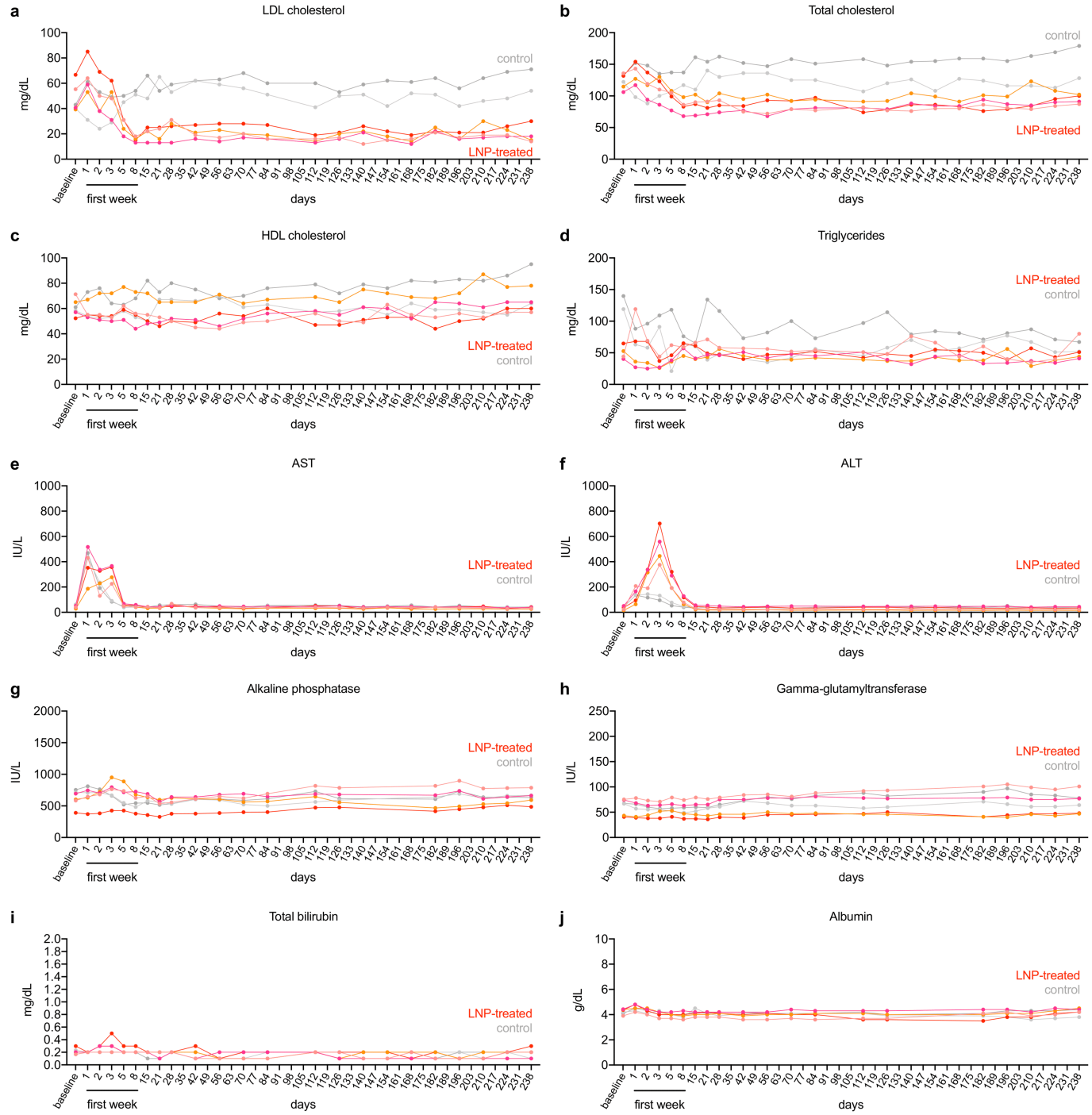

Extended Data Fig. 8 | Long-term pharmacodynamic effects of adenine base editing of *PCSK9* in cynomolgus monkeys. a–**j**, Absolute values of blood levels of LDL cholesterol (**a**), total cholesterol (**b**), high-density lipoprotein (HDL) cholesterol (**c**), triglycerides (**d**), AST (**e**), ALT (**f**), alkaline phosphatase (**g**), γ-glutamyltransferase (**h**), total bilirubin (**i**) and albumin (**j**) in the individual monkeys portrayed in Fig. 3 ($n = 4$ monkeys treated with a dose of 3.0 mg kg^{-1} of an LNP formulation with ABE8.8 mRNA and *PCSK9-1* gRNA, and $n = 2$ monkeys treated with PBS) at various time points up to 238 days after treatment. Shades of red represent LNP-treated monkeys, and shades of grey represent control monkeys.

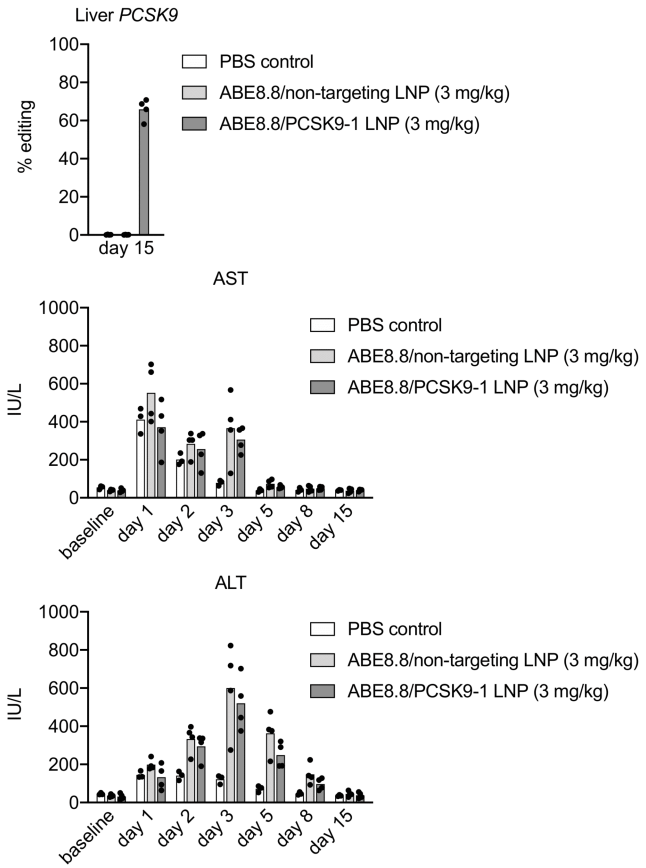

Extended Data Fig. 9 | Additional studies with cynomolgus monkeys receiving a dose of 3.0 mg kg^{-1} of LNPs. Levels of liver editing of the *PCSK9* exon 1 splice-donor adenine base (at day 15), blood AST and blood ALT. $n = 3$ monkeys treated with PBS, $n = 4$ monkeys treated with a dose of 3.0 mg kg^{-1} LNPs containing ABE8.8 mRNA and non-*PCSK9*-targeting gRNA and $n = 4$ monkeys treated with a dose of 3.0 mg kg^{-1} ABE8.8 and *PCSK9-1* LNPs. Bar indicates mean value at each time point.

nature research

Corresponding author(s): Sekar Kathiresan

Last updated by author(s): Mar 26, 2021

Reporting Summary

Nature Research wishes to improve the reproducibility of the work that we publish. This form provides structure for consistency and transparency in reporting. For further information on Nature Research policies, see our Editorial Policies and the Editorial Policy Checklist.

Statistics

For all statistical analyses, confirm that the following items are present in the figure legend, table legend, main text, or Methods section.

n/a	Confirmed	
☐	☒	The exact sample size (*n*) for each experimental group/condition, given as a discrete number and unit of measurement
☐	☒	A statement on whether measurements were taken from distinct samples or whether the same sample was measured repeatedly
☒	☐	The statistical test(s) used AND whether they are one- or two-sided *Only common tests should be described solely by name; describe more complex techniques in the Methods section.*
☒	☐	A description of all covariates tested
☒	☐	A description of any assumptions or corrections, such as tests of normality and adjustment for multiple comparisons
☐	☒	A full description of the statistical parameters including central tendency (e.g. means) or other basic estimates (e.g. regression coefficient) AND variation (e.g. standard deviation) or associated estimates of uncertainty (e.g. confidence intervals)
☒	☐	For null hypothesis testing, the test statistic (e.g. *F*, *t*, *r*) with confidence intervals, effect sizes, degrees of freedom and *P* value noted *Give P values as exact values whenever suitable.*
☒	☐	For Bayesian analysis, information on the choice of priors and Markov chain Monte Carlo settings
☒	☐	For hierarchical and complex designs, identification of the appropriate level for tests and full reporting of outcomes
☒	☐	Estimates of effect sizes (e.g. Cohen's *d*, Pearson's *r*), indicating how they were calculated

Our web collection on statistics for biologists contains articles on many of the points above.

Software and code

Policy information about availability of computer code

Data collection	GraphPad Prism v8.4.3
Data analysis	GraphPad Prism v8.4.3, Primer3 v4.1.0, CRISPResso2 v2.0.31, CRISPOR v4.98, gatk4 v4.1.8.1, STAR v2.7.1a, perbase v0.5.1, R v3.6.2, DESeq2 v1.26.0, trimmomatic v0.39, FLASH v1.2.11, Bowtie2 v2.4.1, samtools v1.10, bedtools v2.25.0, Cas-Designer v1.2

For manuscripts utilizing custom algorithms or software that are central to the research but not yet described in published literature, software must be made available to editors and reviewers. We strongly encourage code deposition in a community repository (e.g. GitHub). See the Nature Research guidelines for submitting code & software for further information.

Data

Policy information about availability of data

All manuscripts must include a data availability statement. This statement should provide the following information, where applicable:

- Accession codes, unique identifiers, or web links for publicly available datasets
- A list of figures that have associated raw data
- A description of any restrictions on data availability

DNA and RNA sequencing data that support the findings of this study have been deposited in the NCBI Sequence Read Archive with the accession code PRJNA716270. All other data supporting the findings of this study (Figs. 1–4, Extended Data Figs. 1–9) are available within the paper and its supplementary information files. The GRCh38 reference human genome (ftp.ncbi.nlm.nih.gov/genomes/all/GCA/000/001/405/GCA_000001405.15_GRCh38/seqs_for_alignment_pipelines.ucsc_ids/GCA_000001405.15_GRCh38_no_alt_analysis_set.fna.gz, ftp://ftp.ensembl.org/pub/release-98/fasta/homo_sapiens/dna/Homo_sapiens.GRCh38.dna.chromosome.{1-22,X,Y,MT}.fa, ftp://ftp.ensembl.org/pub/release-98/fasta/homo_sapiens/dna/Homo_sapiens.GRCh38.dna.nonchromosomal.fa) and Gencode v34 (ftp://ftp.ebi.ac.uk/pub/databases/gencode/Gencode_human/release_34/gencode.v34.primary_assembly.annotation.gtf.gz) and Ensembl v98 (ftp://ftp.ensembl.org/pub/release-98/gtf/homo_sapiens/Homo_sapiens.GRCh38.98.gtf.gz)

annotations were used. The macFas5 cynomolgus monkey reference genome (ftp://ftp.ensembl.org/pub/release-98/fasta/macaca_fascicularis/dna/Macaca_fascicularis.Macaca_fascicularis_5.0.dna.chromosome.{1-20,X,MT}.fa.gz, ftp://ftp.ensembl.org/pub/release-98/fasta/macaca_fascicularis/dna/Macaca_fascicularis.Macaca_fascicularis_5.0.dna.nonchromosomal.fa.gz) was used.

Field-specific reporting

Please select the one below that is the best fit for your research. If you are not sure, read the appropriate sections before making your selection.

☒ Life sciences ☐ Behavioural & social sciences ☐ Ecological, evolutionary & environmental sciences

For a reference copy of the document with all sections, see nature.com/documents/nr-reporting-summary-flat.pdf

Life sciences study design

All studies must disclose on these points even when the disclosure is negative.

Sample size	Sample sizes were determined based on literature precedence for genome-editing experiments (e.g., references 37-39) as well as ethical considerations (using the minimum number of animals needed for experimentation).
Data exclusions	No data were excluded.
Replication	All experiments were repeated at least once, with the exception of the long-term NHP study due to its requirement for outsize resources as well as ethical reasons (using the minimum necessary number of non-human primates). All attempts at replication were successful.
Randomization	Randomization was used when feasible for mouse and non-human primate experiments. An important exception was exclusion of a non-human primate(s) from a treatment group if the genotype at the genome editing site did not match the treatment (i.e., protospacer DNA sequence). Randomization was not used for cellular experiments due to the substantial risk of replicates from different experimental groups being intermixed on the same 24-well plates leading to replicates that were not readily distinguishable being inadvertently misassigned with respect to their experimental groups and confounding the experiments.
Blinding	Although the investigators responsible for group allocation were not blinded to the allocation scheme, they were blinded to group allocation during data collection, and the investigators responsible for analyses were blinded to the allocation scheme (i.e., non-identifying codes were used as sample designations).

Reporting for specific materials, systems and methods

We require information from authors about some types of materials, experimental systems and methods used in many studies. Here, indicate whether each material, system or method listed is relevant to your study. If you are not sure if a list item applies to your research, read the appropriate section before selecting a response.

Materials & experimental systems

n/a	Involved in the study
☒	☐ Antibodies
☒	☐ Eukaryotic cell lines
☒	☐ Palaeontology and archaeology
☐	☒ Animals and other organisms
☒	☐ Human research participants
☒	☐ Clinical data
☒	☐ Dual use research of concern

Methods

n/a	Involved in the study
☒	☐ ChIP-seq
☒	☐ Flow cytometry
☒	☐ MRI-based neuroimaging

Animals and other organisms

Policy information about studies involving animals; ARRIVE guidelines recommended for reporting animal research

Laboratory animals	Male cynomolgus monkeys (Macaca fascicularis) of Cambodian origin that were 2-3 years of age and 2-3 kilograms in weight at the time of study initiation were obtained by and housed at Envol Biomedical or Altasciences. Female C57BL/6J mice were obtained from The Jackson Laboratory and used for experiments at 8-10 weeks of age; the mice were housed at Charles River Accelerator and Development Lab (CRADL) and were maintained on a 12-hour light/12-hour dark cycle, with a temperature range of 65°F to 75°F and a humidity range of 40% to 60%.
Wild animals	No wild animals were used in the study.
Field-collected samples	No field-collected samples were used in the study.
Ethics oversight	The non-human primate studies were approved by the Institutional Animal Care and Use Committees of Envol Biomedical and

Ethics oversight	Altasciences, respectively. The mouse study was approved by the Institutional Animal Care and Use Committee of the Charles River Accelerator and Development Lab (CRADL).

Note that full information on the approval of the study protocol must also be provided in the manuscript.